Ting-Yong Li, Chun-Xia Huang, Lijun Tian, Marina B. Suarez, and Yongli Gao. Variation of $\delta^{13}C$ in plant-soil-cave systems in karst regions with different degrees of rocky desertification in southwest China. *Journal of Cave and Karst Studies*, v. 80, no. 4, p. 212-228. DOI:10.4311/2018ES0107

VARIATION OF $\delta^{13}C$ IN PLANT-SOIL-CAVE SYSTEMS IN KARST REGIONS WITH DIFFERENT DEGREES OF ROCKY DESERTIFICATION IN SOUTHWEST CHINA AND IMPLICATIONS FOR PALEOENVIRONMENT RECONSTRUCTION

Ting-Yong Li[1, 2, C], Chun-Xia Huang[1], Lijun Tian[3], Marina B. Suarez[3], Yongli Gao[3]

Abstract

Speleothem $\delta^{13}C$ has been taken as an indicator of the history of rocky desertification, and changes in $\delta^{13}C$ have been thought to reflect the transition between C3 and C4 surface vegetation types. In this study the $\delta^{13}C$ values of plants, soil organic matter (SOM), dissolved inorganic carbon (DIC) of waters and modern calcite deposits in caves were investigated at five sites with different rocky desertification degree (RDD) in Southwest China. The main results can be summarized as follows: (1) dominant vegetation was the C3 type, with average plant $\delta^{13}C$ values ranging from -26 ‰ to -32 ‰ (V-PDB), and SOM $\delta^{13}C$ values ranging from -20 ‰ to -25 ‰ (V-PDB) for all the sites; (2) large variation for the $\delta^{13}C$ of DIC from drip water and modern calcite deposits in caves, which must be the result of multiple, inorganic factors in the epikarst zone and not the local vegetation type; (3) a proposed conceptual model to demonstrate that the evolution of Asian summer monsoon (ASM) can be recorded in speleothem $\delta^{13}C$ due to changes in epikarst zone hydrological conditions, exerting influence on stable carbon isotopes' fractionation, and not necessarily due to changing vegetation types in the subtropical zone of Southwest China.

Introduction

Karst is one of the most fragile and vulnerable environments because of the low soil formation rate and high permeability of carbonate rocks. Rocky desertification is defined as the transformation of vegetation- and soil-covered karst areas into rocky landscape under the action of natural processes of hydrology and ecology, and through human activities (Yuan 1997; Jiang et al., 2014). The causes for initiation and development of rocky desertification, including the contributions from natural processes and human activities, are still unknown. To prevent and rehabilitate rocky desertification of karst areas, it is essential to know the history of rocky desertification for a specific region.

Speleothems in karst caves record climatic and ecologic information in geochemical proxies, such as the stable isotopes of oxygen and carbon ($\delta^{18}O$ and $\delta^{13}C$), and the concentrations of several elements (Fairchild et al., 2006). $\delta^{13}C$ and $\delta^{18}O$ have been the most popular proxies in the reconstruction of paleoclimate and paleoenvironmental changes (Dorale et al., 1992; Genty et al., 2003; Fairchild et al., 2006). $\delta^{13}C$ of soil CO_2 is controlled by the proportion of biomass from C3 and C4 plants and the CO_2 respiration of soil in different climatic conditions (Cerling, 1984; Mattey et al., 2016). It is considered that the variations of speleothem $\delta^{13}C$ can reflect the changes of regional vegetation, because the different photosynthetic pathways of different plant types result in different $\delta^{13}C$ values: C4 vegetation has much higher $\delta^{13}C$ (typically around -12 ‰), while carbon isotopic composition of C3 vegetation is close to -25 ‰ (McDermott, 2004); the $\delta^{13}C$ of associated speleothems is -6 ‰ to $+2$ ‰ with overlying C4 plants, and -14 ‰ to -6 ‰ with overlying C3 plants (Salomons and Mook, 1986, p. 241–269; McDermott, 2004). However, direct correlation of the speleothem $\delta^{13}C$ with regional vegetation is a simplified or idealized understanding. In reality, complex processes in soil and the epikarst zone will influence the migration of carbon isotopes and disturb the correlation between the speleothem geochemistry and overlying vegetation (Hendy, 1971; Salomons and Mook, 1986, p. 241–269; Coplen et al., 1994; Bar-Matthews et al., 1996; Baker et al., 1997; Fairchild et al., 2006; Frisia et al., 2011). The most recent publications have emphasized the influence of regional, hydrological circulation and the soil humidity balance on stalagmite $\delta^{13}C$ (Li et al., 2007; Liu et al., 2016).

Rocky desertification is a serious ecological and environmental problem in Southwest China (Jiang et al., 2014). In order to understand the origin and history of regional, rocky desertification, research on the mechanism of carbon isotope migration in karst systems, based on cave monitoring, has been carried out (Luo et al., 2009; Li et al., 2011, 2012). As well, reconstruction of the evolution of regional vegetation via the $\delta^{13}C$ records of speleothems has been done (Li et al., 1998). Li et al. (2012) studied the transition of $\delta^{13}C$ signals from overlying plants, soil, and bedrock, in cave water and modern deposits in Furong Cave, Southwest China. However, investigation of the $\delta^{13}C$ characteristics of modern plants and soils in karst regions with different rocky desertification degree (RDD) has been rare.

[1] Chongqing Key Laboratory of Karst Environment, School of Geographical Sciences, Southwest University, Chongqing, 400715
[2] Field Scientific Observation & Research Base of Karst Eco-environments at Nanchuan in Chongqing, Ministry of Land and Resources of China, Chongqing 408435, China
[3] Department of Geological Sciences, University of Texas at San Antonio, San Antonio, TX 78249, USA
[C] Corresponding author: cdlty@swu.edu.cn

In this paper, the organic carbon $\delta^{13}C$ of living plants (including leaves, branches, stems and roots) and soil at five sites with different rocky desertification degree (RDD) in Southwest China was investigated. In addition, the $\delta^{13}C$ of dissolved inorganic carbon (DIC-$\delta^{13}C$) of cave water in three caves was also monitored. This will increase knowledge about modern vegetation of karst areas in subtropical Southwest China, the transition of $\delta^{13}C$ signals in the epikarst zone with different RDD, and provide greater insight for paleoenvironment reconstruction via speleothem $\delta^{13}C$.

Study Area

The most typical karst landscapes in China are concentrated in Southwest China. Four research sites with different RDD were chosen (Nanchuan, Guanling, Liuzhi and Panxian) (Fig. 1, Table 1) and a previous case study above Furong Cave (Wulong County, Chongqing City) (Li et al., 2012) was used as a comparison.

A humid, subtropical monsoon climate prevails in Southwest China, with precipitation in the April to October rainy season accounting for approximately 70-80 % of the annual rainfall (Li et al., 2011, 2014). The average annual temperature is 18.0 °C in Wulong County (above Furong Cave) and 8.0 °C at Jinfo Mountain, Nanchuan district (above Yangkou Cave, based on meteorological data during 2012 to 2017), with the annual rainfall at these locations being 1200 mm and 1348 mm, respectively (Li et al., 2011, 2012). Average annual temperature in Guanling County (above Naduo Cave) is 14.2 °C and the annual rainfall is 1293 mm (Shen et al., 2016). For Panxian County and Liuzhi Special District in Liupanshui City, the annual temperature/rainfall are 11.9 °C/1234 mm and 14.2 °C/1476 mm, respectively (baike.baidu.com). Detailed geographical information, local vegetation, soil thickness of the study areas and host rock thickness above the corresponding caves are presented in Table 1.

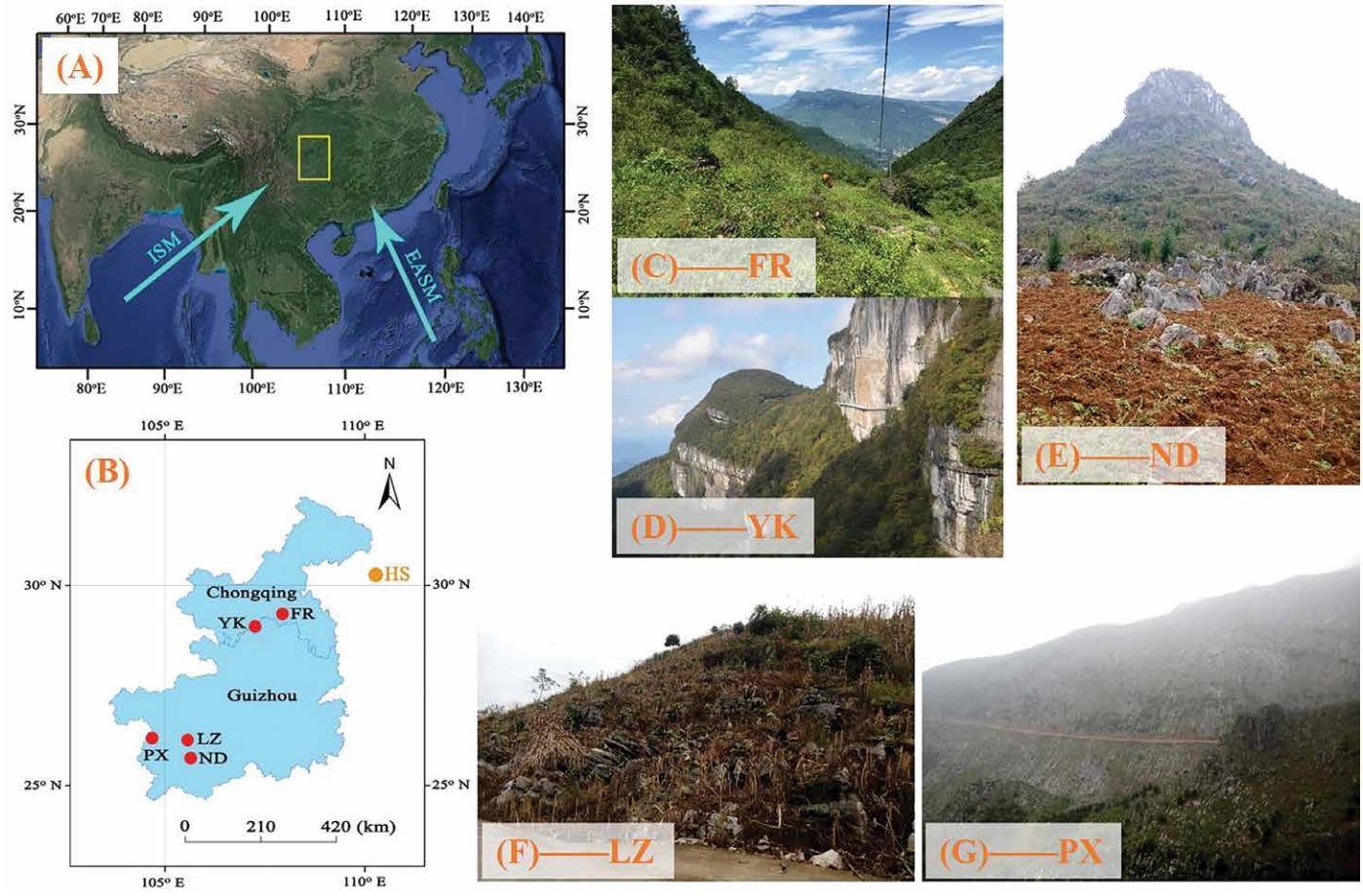

Figure 1. Location map showing the study area and specific sites. (A) The yellow rectangle indicates the study area and cyan arrows denote the directions of the East Asian summer monsoon (EASM) and ISM, which dominate the climate in Eastern and Southern China. (B) Enlarged map of study area. Red solid circles indicate the locations of Furong Cave (FR) (Li et al., 2011, 2012) and Yangkou Cave (YK) (Li et al., 2014a) in Chongqing City; Liuzhi Special District (LZ), Panxian County (PX) and Naduo Cave (ND) in Guizhou province. The brown, solid circle indicates the location of Heshang Cave (HS) (Hu et al., 2008a), which is referred to in this work. Subfigures (C), (D), (E), (F) and (G) show the local vegetation, landform and the situation of rocky desertification at these five study sites. The detailed geographical information of these areas has been described in Table 1.

Table 1. Information about the sampling sites in this study.

Site	Latitude and Longitude	Elevation (m, a.s.l)	Mean annual air temperature, °C	Annual precipitation, mm	Province	Corresponding cave	Soil profiles	Thickness of soil profile, cm	Number of soil subsamples	Number of Plants samples	Vegetation	Rocky desertification degree (RDD)a
Wulong County (Li et al., 2012)	29° 13′ N 107° 54′ E	600–800	17.9	1078	Chongqing	Furong Cave	SA	55	11	27	Arbors and shrubs	No
							SB	25	5			
							SC	87	9			
							SD	64	13			
							SE	78	16			
							SA	55	11			
Nanchuan district	28° 50′ N 107° 20′ E	2150	8.0	1348	Chongqing	Yangkou Cave	JF-1	120	22	24	Arbors and shrubs	No
							JF-2	125	23			
							JF-3	75	14			
Guanling County	25° 48′ N 105° 35′ E	1190	16.2	1268	Guizhou	Naduo Cave	ND	85	13	28	Shrubs and grasses	Light
Liuzi Special District	26° 11′ N 105° 33′ E	1450	14.2	1476	Guizhou	—	LZ-1	12	5	27	Grasses and upland crops	Moderate
							LZ-2	32	8			
							LZ-3	25	5			
Panxian County	26° 14′ N 104° 36′ E	2200	11.9	1234	Guizhou	—	PX-1	12	5	24	Grasses	Severe
							PX-2	29	13			
							PX-3	46	17			

a The classification of rocky desertification (RDD) level based on the rules of Xiong et al., (2002) and Jiang et al., (2014).

Sampling and Analytical Methods

Soil and Plant Samples

Based on the assessment of landform, plant families and vegetation intensity for each research site, one to three soil profiles were dug down to the bedrock, resulting in soil profile depths in the range of 12 cm to 125 cm (Table 1). Soil subsamples were collected at 3 cm to 10 cm intervals from the bottom to the top of each profile, with 125 soil subsamples collected in total (Table 1). The local vegetation was investigated by a 10 m × 10 m quadrat survey and 103 plant samples were collected in total, including the dominant trees, shrubs and grasses (Li et al., 2012, Table 1). For each site, detailed information about the soil profiles, local vegetation and RDD classification are presented in Table 1.

Before analysis for organic carbon $\delta^{13}C$, samples were prepared as follows: Sufficient HCl (5 % v/v) was used to release inorganic carbon from soil subsamples, which were subsequently dehydrated in air at 25 °C and ground into powder with a diameter of less than 50 μm. Plant samples were ultrasonically cleaned for 15 min in deionized water, dried at 50 °C for 48 h, and ground into powder with a diameter less than 150 μm. The detailed procedures are described by Li et al. (2012).

$\delta^{13}C$ analysis of organic matter contained in soil and plant subsamples from Chongqing City were conducted in the School of Geographical Sciences, Southwest University, China. The analytical instrument was the Thermo Delta V Plus, interfaced with a Flash 1200 Elemental Analyzer (EA)/Conflo-III. For the soil and plant samples from Guizhou Province, $\delta^{13}C$ analysis of organic carbon was performed in the Department of Geological Sciences, University of Texas at San Antonio, USA. The analytical instrument was the Thermo Finnigan Delta Plus XP interfaced with a Costech Elemental Analyzer. For both instruments, the analytical error for $\delta^{13}C$ was less than 0.1 ‰ (1σ). All the reported results of $\delta^{13}C$ were given with respect to V-PDB, using internal international standards: USGS-24 graphite ($\delta^{13}C$ = −15.99 ‰), IAEA 600 caffeine ($\delta^{13}C = -27.77$ ‰), ANU Sucrose ($\delta^{13}C = -10.45$ ‰) and Fisher caffeine ($\delta^{13}C = -35.4$ ‰).

CO2 Concentrations of Cave and Soil Air

The CO_2 concentration (pCO_2) of cave air was monitored at drip-water sites (1# through 6#) in Yangkou Cave in Nanchuan district, Chongqing, with results shown in Fig. 2 (Wang et al., 2014). The instrument for determining pCO_2 was infrared device TESTO 535, with a measuring range of 0 ppmV to 9999 ppmV and resolution of 1 ppmV. Three soil profiles from above Yangkou Cave (JF-1, JF-2 and JF-3) were monitored for the pCO_2 of soil air at depths of 20 and 50 cm. The pCO_2 was determined using the Komyo Rikagaku kogyo K.K with AP-20 aspirating pump and 126SA test tube, which had a measuring range of 100 ppmV to 50,000 ppmV and resolution greater than 50 ppmV.

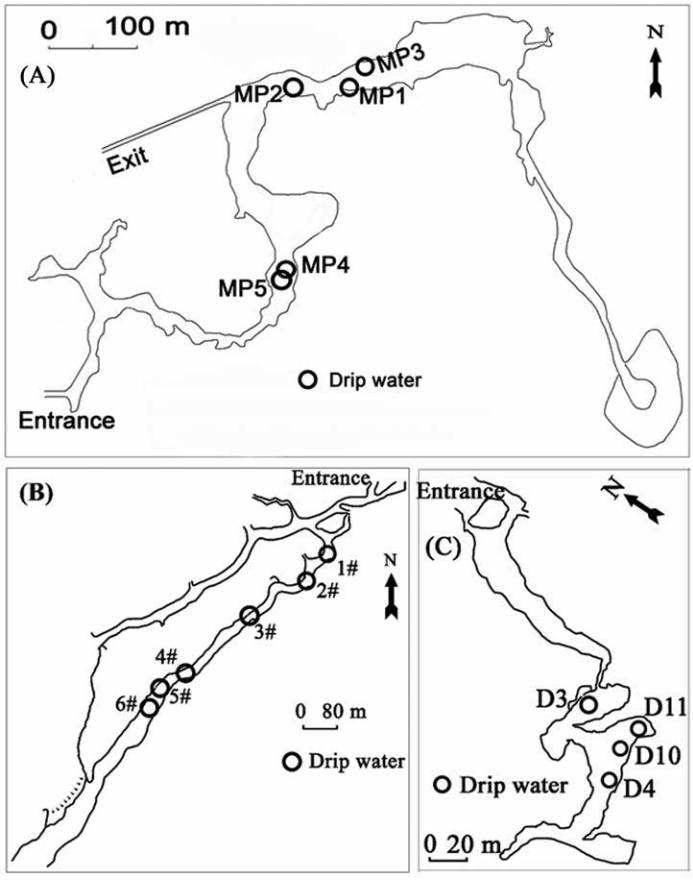

Figure 2. Sketch map of Furong Cave, Yangkou Cave and Naduo Cave and the distribution of the drip-water monitoring sites in the caves. These maps were modified from: (A) Furong Cave (Li et al., 2011); (B) Yangkou Cave (Wang et al., 2014); (C) Naduo Cave (Shen et al., 2016).

Discharge Rate of Drip Water and Temperature of Cave Air

The discharge rate of the six drip water sites (#1 through #6) in Yangkou Cave was monitored. Depending on the water drip rate, the drip water was collected using 10 mL or 100 mL cylinders; the top of each cylinder had a funnel shape with 9 cm diameter. The volume of water collected in one minute was taken to reflect the discharge rate of the drip water (mL/min), and these *in situ* measurements were conducted monthly.

In the period from February 2012 to June 2014, the air temperature in the cave at about 5 m by site 3# was continuously recorded at 2 h intervals using the U12-011 temperature recorder (Onset company, USA), with an error of ±0.1 °C. Data were downloaded via HOBO software every month.

DIC-δ13C in Cave Water

The DIC-$\delta^{13}C$ variation of drip water at six sites in Yangkou Cave (1# through 6#) was monitored. *In situ* sampling of drip water was conducted monthly in the period from July 2013 to October 2015. Collecting time for drip water varied in the range of 2 s to 50 min, based on the drip rate at the specific drip site and the month. To

Table 2. $\delta^{13}C$ and $\delta^{18}O$ values of modern deposits in Yangkou Cave, Jinfo Mts. Chongqing.

Sample	$\delta^{13}C$, ‰	$\delta^{18}O$, ‰
modern-1	−6.7	−6.8
modern-2	−6.3	−6.8
modern-3	−5.4	−6.0
modern-4	−8.4	−7.6
modern-5	−6.3	−7.1
modern-6	−6.9	−7.2
modern-7	−7.8	−7.4
Mean	−6.8	−7.0
Std. dev.	1.0	0.5

water (20 mL) collected from each monitoring site, saturated aqueous $HgCl_2$ solution (0.2 mL) was added instantly to avoid potential isotopic fractionation by the effect of microorganisms. Water samples were sealed tightly and stored in the laboratory refrigerator at 5 °C. CO_2 for the measurement of the DIC was produced by the chemical reaction of phosphoric acid with the water sample. The DIC-$\delta^{13}C$ analyses of water samples were performed in the School of Geographical Sciences, Southwest University, China, using the Thermo Delta V Plus interfaced with the Thermo Gas Bench automated apparatus, with an analytical error of less than 0.2 ‰ (1σ).

For Furong Cave, located in Wulong County, Chongqing (Fig. 1), the DIC-$\delta^{13}C$ of cave water from the published data by Li et al. (2012) was used (Fig. 2A). For Naduo Cave, located in Guanling County, Guizhou Province (Fig. 1), the DIC-$\delta^{13}C$ of cave water from the published data by Shen et al. (2016) was used (Fig. 2C). There were no caves in the sites of Liuzi Special District and Panxian County, Guizhou province (Table 3).

$\delta^{13}C$ of Cave "modern deposits" and Bedrock

Glass plates were placed under the six drip-water sites in Yangkou Cave to collect modern deposits, as was done in Furong Cave (Li et al., 2011, 2012). Only the deposits on artificially-placed substrates under drip water are accurate modern deposits. However, as there was no visible deposit on the plates through the monitoring period over several years, powders were scraped (less than 1 mm in depth) from the tops of stalagmites under drip sites without signs of

Table 3. Changes of $\delta^{13}C$ in karst regions at different RDD, Southwest China.

Sites	Correspond cave	Thickness of Host rock, m	RDD	Average $\delta^{13}C$, ‰					
				Plants	Soils, SOM	Bedrock	DIC of drip water	Modern deposits	Note
Wulong County	Furong Cave	300−500	No	−31.8 ± 4.3a	−22.0 ± 1.4a	−1.1 ± 1.3	−11.1 ± 0.6a	−10.5 ± 0.7a	Li et al. (2012)a
Nanchuan District	Yangkou Cave	50−100	No	−28.9 ± 1.8	−24.6 ± 0.5	3.9 ± 0.5	−3.0 ± 2.7	−6.8 ± 1.0	This study
Guanling County	Naduo Cave	30−85	Light	−26.2 ± 7.4	−20.6 ± 0.9	1.5 ± 1.4	−5.3 ± 2.2b	−6.5 ± 1.4	Shen et al. (2016)b
Liuzhi Special District	NCCc	···	Moderate	−27.5 ± 5.5	−19.9 ± 1.3	−0.2 ± 0.0 (n=1)	···	···	This study
Panxian County	NCCc	···	Severe	−26.5 ± 4.2	−21.2 ± 1.5	3.6 ± 0.9	···	···	This study

a Referred from Li et al. (2012)
b Referred from Shen et al. (2016)
c NCC = no corresponding cave identified but plants, soil, and bedrock samples were collected.

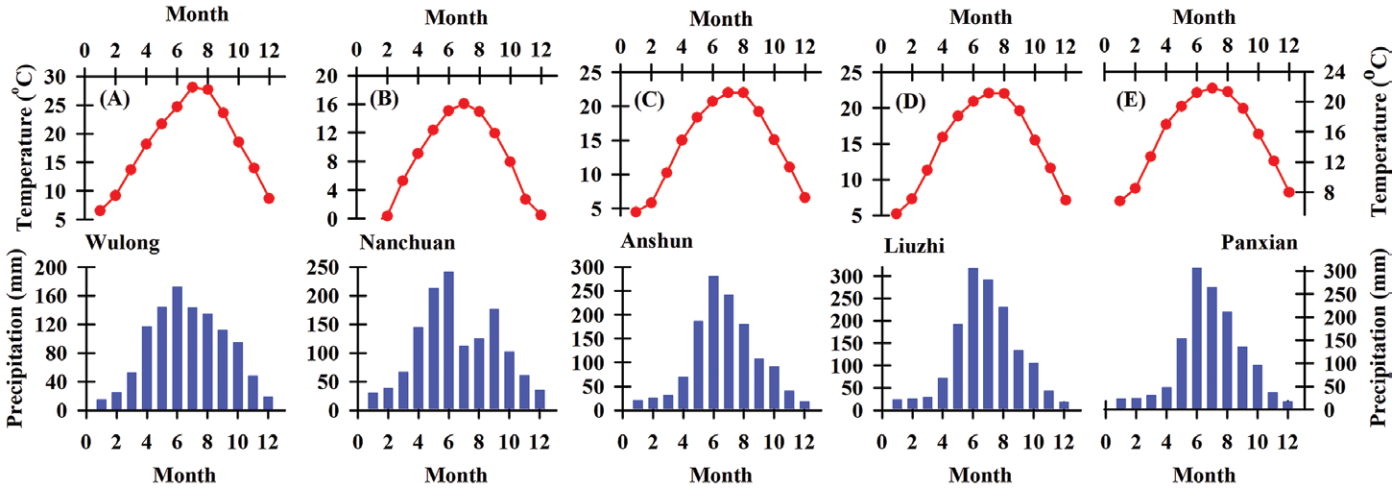

Figure 3. Monthly air temperature (°C) and precipitation (mm) for the study sites. (A) Wulong County (the location of Furong Cave), based on meteorological data from 2005 to 2016). (B) Jinfo Mt., Nanchuan District (the location of Yangkou Cave), based on meteorological data from 2012 to 2017. (C), (D), and (E) Anshun (the location of Naduo Cave), Liuzhi and Panxian, respectively, based on meteorological data from 1988 to 2010 from the meteorological data center of China Meteorological Administration (http://data.cma.cn/).

erosion or dissolution. Otherwise, visible, fresh deposits were collected from the surface of collapsed bedrock with drip water instead. These artificial, modern deposits would not influence the relationship between the DIC-$\delta^{13}C$ of drip water and RDD, because the relationship between drip water and deposit $\delta^{13}C$ is influenced by cave-related factors (e.g. ventilation, CO_2 degassing). Whereas the relationship between DIC-$\delta^{13}C$ of drip water and RDD is influenced by the factors in soil and the host rock. Analysis of $\delta^{13}C$ in the "modern deposits" samples was performed in the School of Geographical Sciences, Southwest University, China, using the Kiel IV carbonate device and Thermo Delta V Plus, with analytical error of below 0.1 ‰ (1σ). For each study area (Fig. 1), from above the cave and from near the drip-water sites in the cave, several blocks of bedrock were collected, broken by hammer and powder scraped from the fresh surface. The $\delta^{13}C$ content of this bedrock powder was determined using the same instruments as for the modern deposit samples.

Results

$\delta^{13}C$ of Plants

Twenty-four plant samples (classified as 24 species from 20 families) were collected from above Yangkou Cave (Jinfo Mt., Chongqing) (Supplementary Table 1). All of these plants were dominant species in the karst area of Southwest China. The $\delta^{13}C$ values of the plants ranged from −25.0 ‰ to −32.2 ‰, with the average being −28.9 ‰ ± 1.8 ‰. Twenty-eight plant samples were collected from above Naduo Cave (Guanling County, Guizhou province), with $\delta^{13}C$ values ranging from −11.2 ‰ to −32.2 ‰, with an average of −26.2 ‰ ± 7.4 ‰ (Supplementary Table 2). For the 27 plant samples collected in Liuzhi Special District, the $\delta^{13}C$ values ranged from −12.0 ‰ to −32.4 ‰ with an average of −27.5 ‰ ± 5.5 ‰ (Supplementary Table 3). Of the 24 plant samples collected in Panxian County, the $\delta^{13}C$ values ranged from −13.1 ‰ to −29.8 ‰, and the average was −26.5 ‰ ± 4.2 ‰ (Supplementary Table 4).

$\delta^{13}C$ of soil organic matter (SOM)

Three soil profiles were dug above Yangkou Cave, named JF-1, JF-2 and JF-3 at depths of 120 cm, 125 cm, and 73 cm, respectively (Table 1). For each profile, the average $\delta^{13}C$ values of SOM ($\delta^{13}C_{SOM}$) were −24.4 ‰ ± 0.5 ‰, −24.9 ‰ ± 0.3 ‰, and −24.2 ‰ ± 0.4 ‰ (Fig. 4A; Supplementary Table 5), respectively. The soil profile above Naduo Cave was 85 cm in depth (Table 1), with an average $\delta^{13}C_{SOM}$ of −20.6 ‰ ± 0.9 ‰ (Fig. 4B; Supplementary Table 6). The average $\delta^{13}C_{SOM}$ values of three soil profiles in Liuzhi Special District were −19.8 ‰ ± 0.4 ‰, −19.2 ‰ ± 1.5 ‰ and −21.3 ‰ ± 0.4 ‰, and the average was −19.9 ‰ ± 1.3 ‰ for all soil samples (Fig. 4C; Supplementary Table 7). The average $\delta^{13}C_{SOM}$ values of three soil profiles in Panxian County were −23.0 ‰ ± 0.7 ‰, −21.5 ± 1.7 ‰, and −20.4 ‰ ± 0.9 ‰ and the average was −21.2 ‰ ± 1.5 ‰ for all of these soil samples (Fig. 4D; Supplementary Table 8).

CO_2 Concentration of Soil Air above Yangkou Cave

The CO_2 concentration of soil air above Yangkou Cave changed seasonally in the range of 200-6800 ppmV, generally with higher values in summer and autumn months and lower values in winter and spring months (Fig. 5). Depth of soil profiles JF-1 and JF-2 were 120 cm and 125 cm, respectively, deeper than that of profile JF-3 at 70 cm (Table 1). Correspondingly, the average CO_2 concentration of soil air in JF-1 and JF-2 was 950 ppmV and 1300 ppmV, respectively, higher than in JF-3 at 800 ppmV.

CO_2 Concentration of Cave Air in Yangkou Cave

For the six cave air CO_2-monitored sites (1#-6#, as drip water sites), the CO_2 concentration changed in the range of 308 ppmV to 554 ppmV, 326 ppmV to 654 ppmV, 316 ppmV to 800 ppmV, 333 ppmV to 622 ppmV, 346 ppmV to 781 ppmV and 312 ppmV to 544 ppmV, with an average of 388 ppmV, 412 ppmV, 446 ppmV, 402 ppmV, 445 ppmV,

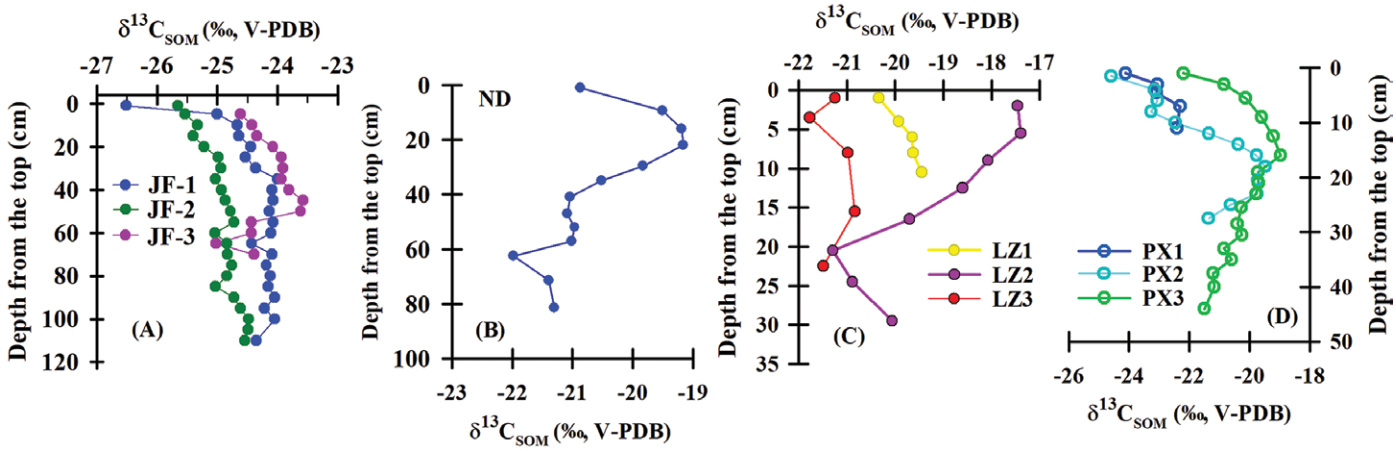

Figure 4. The $\delta^{13}C$SOM of soil profiles in: (A) Jinfo Mt., above Yangkou Cave, (B) Anshun country, the location of Naduo Cave, (C) Liuzhi Special District, and (D) Panxian County in Guizhou province.

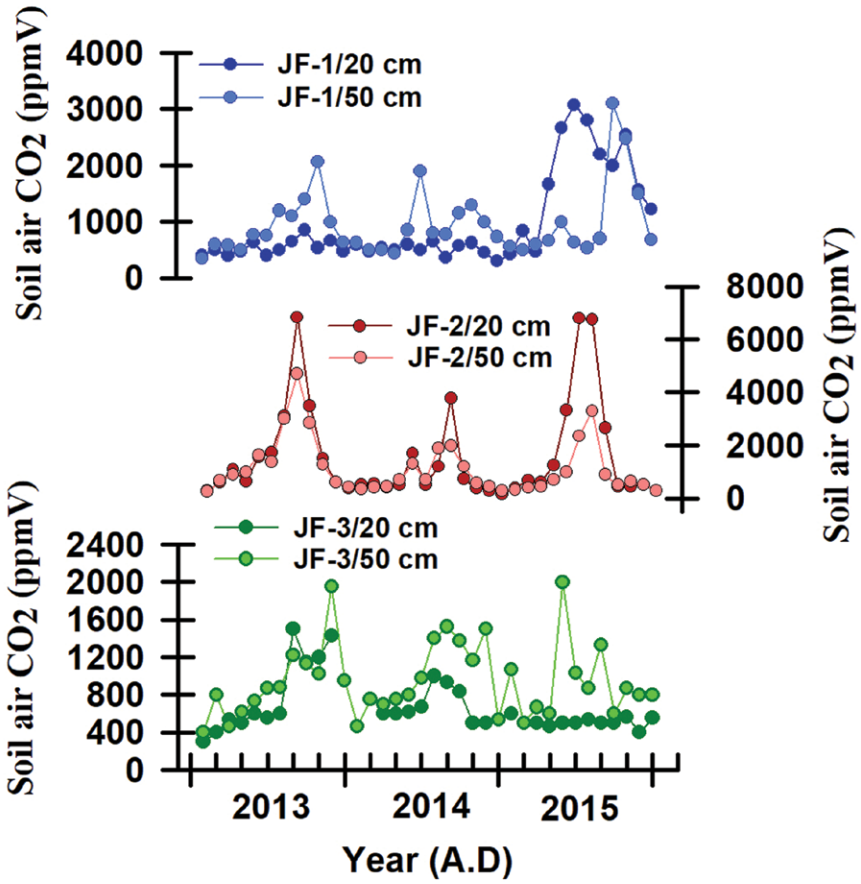

Figure 5. Monthly changes in soil air CO_2 concentration at different depths for the three soil profiles in Jinfo Mt., above Yangkou Cave.

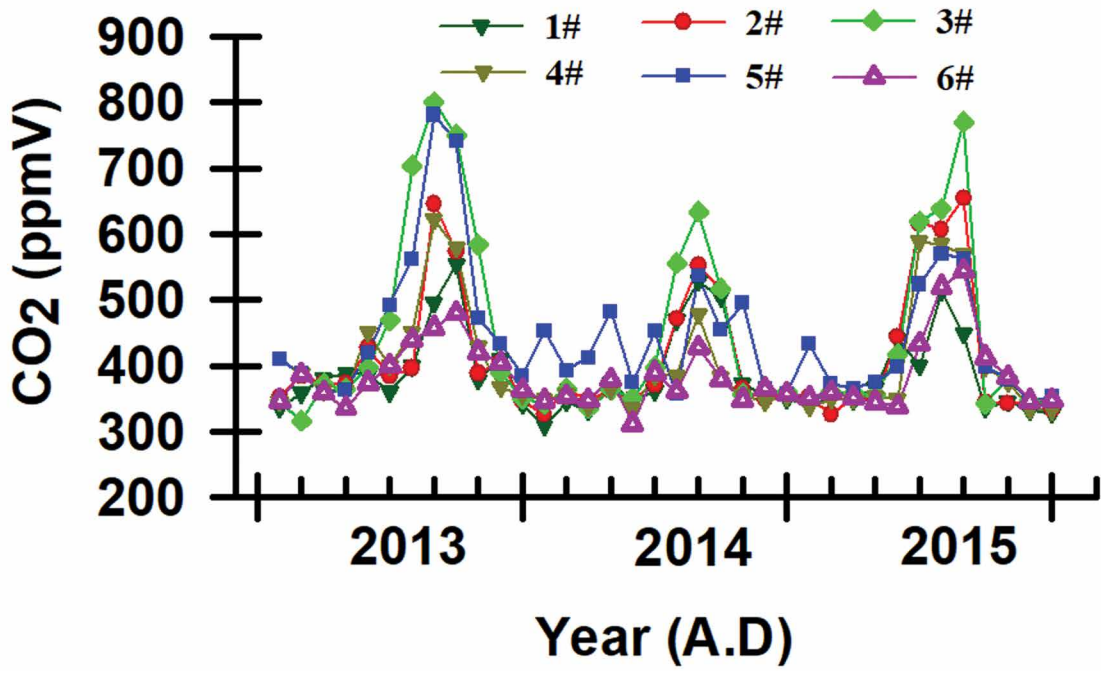

Figure 6. Monthly changes of cave air CO_2 concentration for the six drip-water monitoring sites in Yangkou Cave.

and 385 ppmV, respectively. There were obvious seasonal changes of cave air CO_2 concentration in Yangkou Cave, with higher values in the 600 ppmV to 800 ppmV range in summer months and lower values in the 300 ppmV to 400 ppmV range in winter and spring months (Fig. 6).

The relatively low soil CO_2 concentration above Yangkou Cave and air CO_2 concentration in Yangkou Cave were in contrast with the global average concentration of atmospheric CO_2 (~400 ppmV). This could possibly be attributed to analytical uncertainty (i.e., 50 ppmV for soil CO_2). Additionally, the high elevation above Yangkou Cave, which is more than 2,100 m a.s.l. and frequently frozen in winter months because of the low air temperature, resulted in significant depression of soil CO_2 production. Despite this phenomenon, the seasonal changes of CO_2 concentration in the soil and in the cave were clear.

Discharge Rate Variation of Drip Water in Yangkou Cave

The average discharge rate for the six drip-water sites (1#-6#) in Yangkou Cave were 178.6 mL/min, 141.5 mL/min, 15.4 mL/min, 2.8 mL/min, 6.9 mL/min, and 96.3 mL/min, respectively. Except at site 5#, there was no obvious seasonal change in the discharge rate (Fig. 7). For all the drip sites, the discharge changed in the range of 2.6 mL/min and 898.0 mL/min, 17.0 mL/min and 269.0 mL/min, 5.0 mL/min and 28.0 mL/min, 0.4 mL/min and 22.0 mL/min, 1.0 mL/min and 27.0 mL/min, and 3.9 mL/min, and 322.0 mL/min, respectively. This huge range in the change of discharge rate indicated that most of the drip waters monitored in Yangkou Cave were fissure water and responded relatively quickly to local precipitation, especially for drip sites 1#, 2# and 6# (Fig. 7).

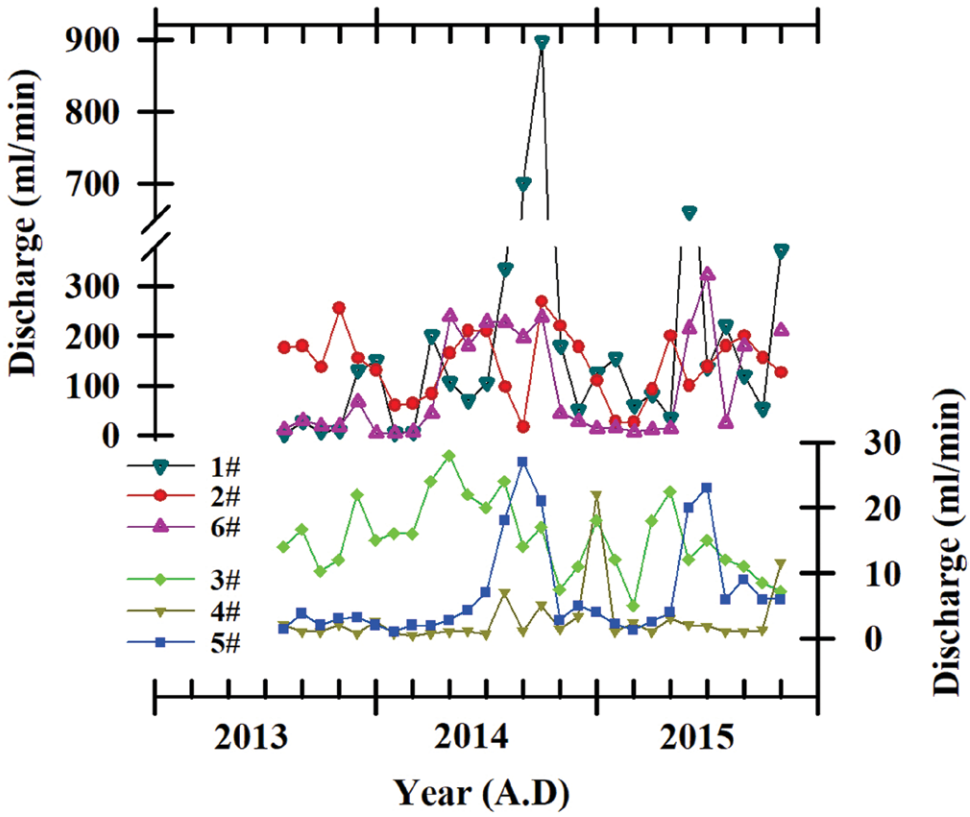

Figure 7. Monthly changes of the discharge rate for the six drip-water monitoring sites in Yangkou Cave.

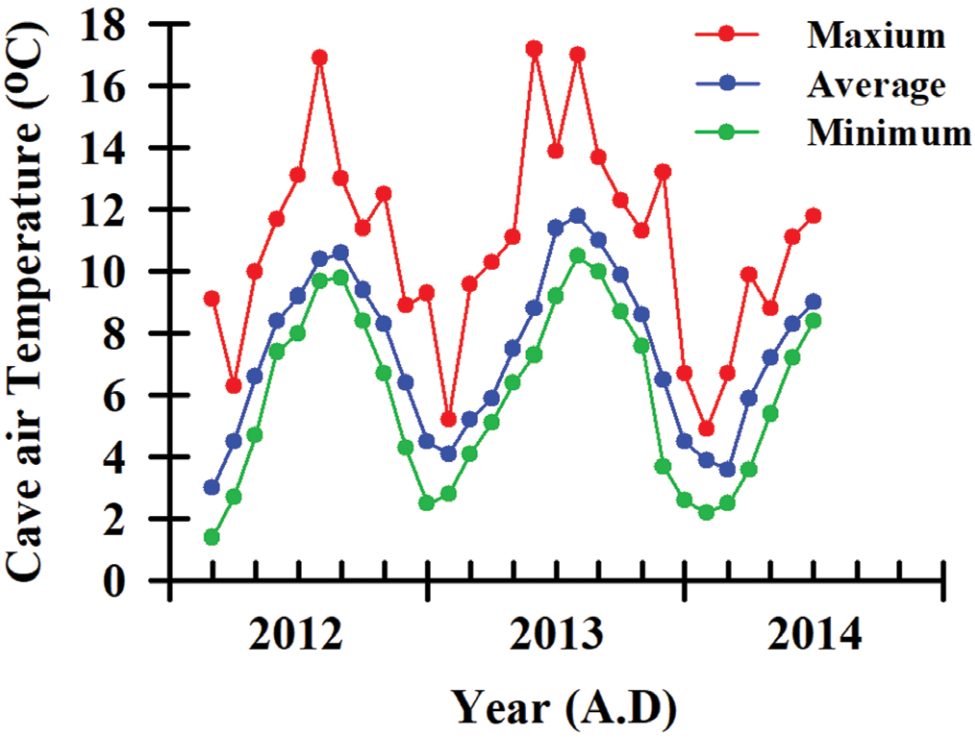

Figure 8. Monthly changes of cave air temperature, monitored at about five m from site 3# in Yangkou Cave (Fig. 2C).

Air Temperature in Yangkou Cave

In the period from February 2012 to June 2014, the air temperature in Yangkou Cave fluctuated in the range of 1.4 °C – 17.2 °C (Fig. 8), with higher temperatures in the summer months and lower values in winter months, similar to the seasonal change of regional air temperature outside the cave (Fig. 3B). For the whole monitoring period, the monthly mean air temperature in Yangkou Cave was 7.4 °C, close to the value of 7.5 °C, reported by Li et al. (2014a).

$\delta^{13}C$ of DIC, Bedrock and Modern Deposits

The average DIC-$\delta^{13}C$ values for the six drip-water sites (1#-6#) in Yangkou Cave were −5.1 ‰ ± 2.3 ‰, −3.0 ‰ ± 1.9 ‰, −5.8 ‰ ± 1.8 ‰, −0.3 ‰ ± 1.0 ‰, −0.5 ‰ ± 1.4 ‰, and −1.8 ‰ ± 1.8 ‰, respectively (Fig. 9). The great fluctuation in the ranges of drip water DIC-$\delta^{13}C$ (4 ‰ to 10 ‰) in Yangkou Cave (Fig. 9) should partially be attributed to the relatively open channel of the cave and the considerable cave ventilation effect (Fairchild et al., 2006), as partly indicated by the huge magnitude of air temperature fluctuations in Yangkou Cave (1.4 to 17.2 °C) (Fig. 8). Other potential reasons for the irregular change in drip water DIC-$\delta^{13}C$ in Yangkou Cave could include the seasonal change of soil CO_2 production and the equilibrium between soil water and soil CO_2 (Baker et al., 1997). Both are closely related to changeable precipitation and soil hydrological conditions.

Sixteen subsamples of bedrock were collected in total, 11 in Yangkou Cave and five out of the cave, with the average $\delta^{13}C$ values being 4.1‰ and 3.5‰, respectively. For all the bedrock subsamples, the average $\delta^{13}C$ was 3.9 ‰ ± 0.5 ‰ (Supplementary Table 9). The $\delta^{13}C$ values of seven “modern deposit” subsamples collected in Yangkou Cave, ranged from −5.4 ‰ to −8.4 ‰, with an average value of −6.8 ‰ ± 1.0 ‰ (Table 3).

Discussion

Differences in $\delta^{13}C$ of Regional Plants

For all sites mentioned in this study, Wulong, Nanchuan, Guanling, Liuzhi and Panxian, the average $\delta^{13}C$ of local plants was −31.8 ‰ ± 4.3 ‰ (Li et al., 2012), −28.9 ‰ ± 1.8 ‰, −26.2 ‰ ± 7.4 ‰, −27.5 ‰ ± 5.5 ‰, and −26.5 ‰ ± 4.2 ‰, respectively (Table 3).

The average $\delta^{13}C$ value of the plants above Naduo Cave (in Guanling County), −26.2 ‰, was close to that of plants above Yangkou Cave (−28.9 ‰). The relatively large standard deviation (7.4 ‰ for Naduo Cave vs. 1.8 ‰ for Yangkou Cave), was attributed to four species above Naduo Cave: *Pogonatherum paniceum, Imperata cylindrica, Sorghum bicolor* and *Capillipedium assimile*, with $\delta^{13}C$ values higher than -13‰ (Supplementary Table 2). *Sorghum bicolor* is a crop introduced from Northern China. *Pogonatherum paniceum, Imperata cylindrica* and *Capillipedium assimile* are local grasses; these account for an especially small proportion (< 3%) of local biomass, based on the field investigation. Exclusion of these four species resulted in an average $\delta^{13}C$ for plants above Naduo Cave of −29.9 ‰ ± 1.6 ‰.

For Liuzhi Special District, the species of *Arthraxon hispidus, Imperata cylindrica* and *Zea mays*, which are Gramineae plants, had higher $\delta^{13}C$ values of around −12 ‰ to −13 ‰ (Supplementary Table 3). Exclusion of these three species resulted in an average $\delta^{13}C$ for the other 24 plant samples of −29.4 ‰ ± 1.6 ‰. *Zea mays* is a crop and *Arthraxon hispidus* and *Imperata cylindrical* are grasses. For most local plants in Liuzhi, the $\delta^{13}C$ value is around −29 ‰.

For Panxian County, the Gramineae grass species *Imperata cylindrica* and *Arthraxon hispidus*, with higher $\delta^{13}C$ values of −13.4 ‰ and −13.1 ‰, respectively, accounted for a relatively small proportion of local, total biomass. Exclusion of these two species resulted in an average $\delta^{13}C$ for the other 22 plant samples of −27.7 ‰ ± 1.1 ‰, with all $\delta^{13}C$ values below −25 ‰ (Supplementary Table 4).

In summary, for most of the present vegetation in these four study sites, the average $\delta^{13}C$ of plants consistently matched the $\delta^{13}C$ distribution of modern C3 photosynthesis vegetation (−20 ‰ to −35 ‰) (Dienes, 1980, p. 320–406; McDermott, 2004). In other words, at present, severe rocky desertification in Panxian County has not changed the dominance of C3 vegetation. This observation is essentially different to previous opinion, which argued that the evolution of rocky desertification in southwest China will change C3/C4 vegetation and finally result in changes to speleothem $\delta^{13}C$ (Zhang et al., 2006).

Variation of $\delta^{13}C_{SOM}$ in Soils

For soil profiles JF-1 and JF-2 above Yangkou Cave, the $\delta^{13}C_{SOM}$ values were steady, with variation of about 0.5 ‰ below a depth of about 40 cm. Additionally, from the top to the bottom of the soil profiles, the $\delta^{13}C_{SOM}$ values tended to increase (Fig. 4A), which was consistent with the trend in $\delta^{13}C_{SOM}$ values above Furong Cave (Li et al., 2012) arising from the fractionation of stable carbon isotopes, due to plant decomposition (Trumbore, 2000). The lowest $\delta^{13}C_{SOM}$ values at the top of the soil profiles, as low as −28.9 ‰ ± 1.8 ‰ (Table 3), were attributed to the relatively large amount of undecomposed plants at the top of the soil profile. However, profile JF-3 showed a reverse of this trend from a depth of 45 cm, with a higher $\delta^{13}C_{SOM}$ value by about 1.5 ‰ at the depth of 65 cm (Fig. 4A). This abnormal phenomenon was attributed to the uneven distribution of plant roots and residues, or some disturbance of the soil layers.

Above Naduo Cave, the $\delta^{13}C_{SOM}$ values increased with growing depth for the top 22 cm section of the soil profile, but became relatively lower at depths of 22 cm to 41 cm (Fig. 4B). At deeper than 41 cm, the $\delta^{13}C_{SOM}$ values were around −21 ‰, except for an excursion of ~1 ‰ at a depth of 63 cm (Fig. 4B). This distribution of $\delta^{13}C_{SOM}$ values along the soil profile was similar to the characteristics of soil profile JF-3 above Yangkou Cave (Fig. 4A), as explained above.

From the top to bottom, the $\delta^{13}C_{SOM}$ of profiles LZ1 and LZ3 remained steady around their average values, with a variation amplitude of about 1 ‰ (Fig. 4C). The $\delta^{13}C_{SOM}$ of profile LZ2 decreased by 3.8 ‰ from the top to a depth of 20.5 cm, and reversed to increase by 1‰ at the bottom. Maize (*Zea mays*), which is a C4 plant ($\delta^{13}C$ = −12.3 ‰) and a typical crop in southwest China, can grow even in karst regions with severe, rocky desertification because of its drought tolerance. Accordingly, one additional soil sample was collected from maize land in Liuzhi Special District, and the $\delta^{13}C_{SOM}$ test result was −20.9 ‰. Therefore, the development of human agricultural activities and the planting of maize in karst regions had no significant effect on the enrichment of the value of $\delta^{13}C_{SOM}$.

Generally, the $\delta^{13}C_{SOM}$ values of PX1 increased from the top to the bottom of the soil profile. Both the PX2 and PX3 profiles showed an increase in $\delta^{13}C_{SOM}$ values from the top to a depth of 18 cm and 16 cm, respectively, and then decreased by 1.9 ‰ and 2.5 ‰, respectively, to the bottom (Fig. 4D). This was similar to the $\delta^{13}C_{SOM}$ changes in the soil profiles above Naduo Cave (Fig. 4A) and for LZ2 in Liuzhi Special District (Fig. 4C), which was attributed to the rapid water loss and soil erosion in the karst rocky desertification area (Jiang et al., 2014). This led to the relatively fast migration of surface SOM and relatively lower $\delta^{13}C_{SOM}$ values into the deep soil layers.

Relatively Higher DIC-$\delta^{13}C$ in Yangkou Cave

Because of the large cave opening and over 10 m high/wide tunnel of Yangkou Cave, the monthly average air temperature in the deepest chamber of this cave ranged from 1.4 to 17.2 °C during the period of February 2012 to June 2014 (Fig. 8). Seasonal temperature changes influence the cave ventilation, accounting for the disequilibrium fraction-

ation of stable, carbon isotopes with the degassing of CO_2 (Spötl et al., 2005). The relatively higher DIC-$\delta^{13}C$ of drip water in Yangkou Cave could be explained by incomplete isotopic equilibrium between soil CO_2 and percolating H_2O, due to relatively short water-soil residence times (Baker et al., 1997), as indicated by the relatively fast discharge of drip waters (except at site #4) (Fig. 7). Another possible reason is the relatively lower biological activity in the overlying soils because of the higher elevation (2,150 m a.s.l) and lower temperature, which result in a lower soil CO_2 concentration (Fig. 5). For example, the maximum soil CO_2 concentrations above Yangkou Cave were about 3200 ppmV, 7000 ppmV, and 2000 ppmV for JF-1, JF-2, and JF-3 soil profiles, respectively (Fig. 5). In contrast, the maximum soil CO_2 concentration above Furong Cave was more than 13,000 ppmV in the months of July and August. The higher DIC-$\delta^{13}C$ values and lower discharge rate of site #4 may be attributed to the fractionation of stable isotopes by prior calcite precipitation (PCP) due to the long residence of groundwater (Fairchild et al., 2006).

Systematic Variation of $\delta^{13}C$ for Yangkou Cave

The average $\delta^{13}C_{SOM}$ value above Yangkou Cave was −24.6 ‰ ± 0.5 ‰, about 4.4 ‰ higher, compared to the average $\delta^{13}C$ value of the plants above Yangkou Cave, which was −28.9 ‰ ± 1.8 ‰ (Table 3). Above Furong Cave, the average $\delta^{13}C_{SOM}$ value was −21.5 ‰, which was 11.6 ‰ higher than the $\delta^{13}C$ value of local plants (−31.8 ‰) (Li et al., 2012). The relatively small difference in soil and plant $\delta^{13}C$ above Yangkou Cave was attributed to the higher altitude (2,150 m a.s.l) (Table 1), lower temperature, greater precipitation and higher regional humidity, which result in relatively lower decomposition of SOM and preserve the negative $\delta^{13}C$ information of local plants.

The average $\delta^{13}C$ value of the "modern deposits" in Yangkou Cave was −6.8 ‰ ± 1.0 ‰ (Table 3), lower than the average DIC-$\delta^{13}C$ value of drip water, which was 3.0 ‰ ± 2.7 ‰ (Table 3). It must be reiterated that the scraped modern deposits of Yangkou Cave in this study were temporal mixing deposits (months or years), not the deposits strictly precipitated from the contemporaneous drip water, as described in section 3.5. Considering the DIC-$\delta^{13}C$ of drip water changes greatly (Fig. 9), if most of the collected "modern deposits" precipitated from the water had relatively lower DIC-$\delta^{13}C$ values, this could reasonably explain why the $\delta^{13}C$ values of the "modern deposits" were seemingly even lower than those of DIC in drip water. Additionally, the average value of −6.8 ‰ for the modern deposits in Yangkou Cave was within the range of −14 ‰ to −6 ‰ for speleothems with overlying C3 vegetation (McDermott, 2004). The relatively higher carbon isotope signature should be attributed to multiple factors, such as the rapid filtering of percolating H_2O (Fig. 7), resulting in non-equilibrium of isotopes between soil water and soil CO_2 (Baker et al., 1997), and rapid degassing of CO_2 for drip waters because of the strong ventilation (Fig. 8) (McDermott, 2004). Nevertheless, even considering the overlying dominance of C3 plants, the $\delta^{13}C$ values of the modern deposits in Yangkou Cave were relatively high.

Systematic Variation of $\delta^{13}C$ for Naduo Cave

The DIC-$\delta^{13}C$ of drip waters for four drip sites in Naduo Cave ranged from 0.6 ‰ to −10.4 ‰ with an average of −5.3 ‰ ± 2.2 ‰, based on data published by Shen et al. (2016). This massive DIC-$\delta^{13}C$ range in the Naduo Cave drip waters was attributed to seasonal changes in soil CO_2, which, presented by the CO_2 in cave air, ranged from 300 ppmV to 1700 ppmV. It was also ascribed to the difference in length and pathways of groundwater for each drip site (Shen et al., 2016). The $\delta^{13}C$ of modern deposits in Naduo Cave changed in the range of −4.3 ‰ to −8.6 ‰ and the average being −6.5 ‰ ± 1.4 ‰ (Table 3). So, for Naduo Cave, the $\delta^{13}C$ is increased by 5.6 ‰ and 15.3 ‰, from local plants to SOM and from SOM to drip water DIC, respectively. The average $\delta^{13}C$ of modern deposits in Naduo Cave were relatively lower compared with the average of DIC in drip waters, like those in Yangkou Cave. Considering the $\delta^{13}C$ of bedrock above Naduo Cave was 1.5 ‰, this phenomenon was attributed to the asynchrony of the modern deposits and drip water. In other words, most "modern deposits" precipitated from drip water with relatively lower DIC-$\delta^{13}C$ value, similar to as discussed with systematic variation in Yangkou Cave.

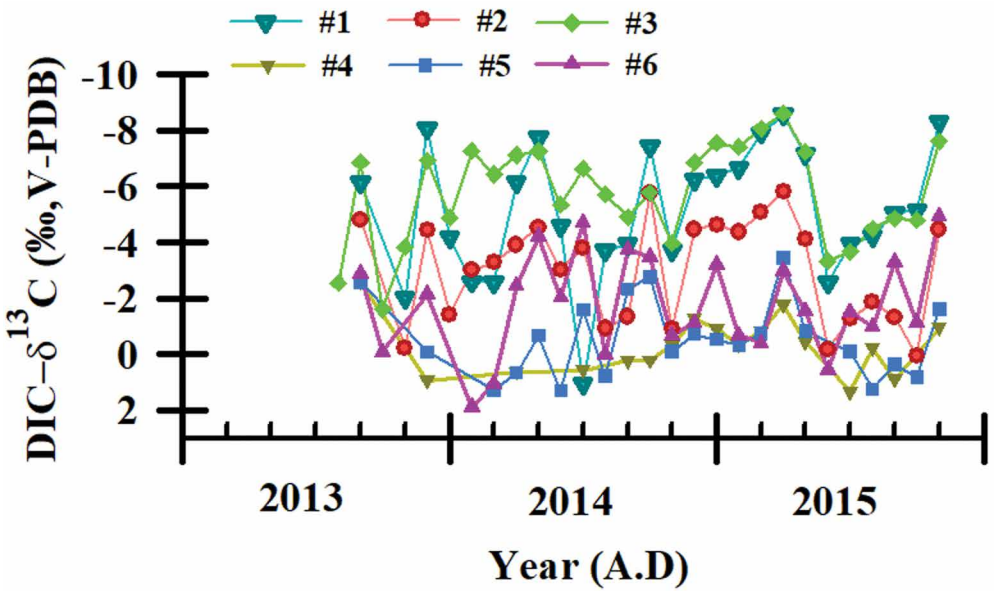

Figure 9. The drip-water DIC-$\delta^{13}C$ values in Yangkou Cave for the six drip-water sites (1# to 6#).

Changes of $\delta^{13}C$ in Karst Regions with Different RDD

There were some differences in the $\delta^{13}C$ of plants in the five karst areas discussed in this study. The lowest average plant $\delta^{13}C$ (−31.8 ‰) presented above Furong Cave, and the highest value (−26.2 ‰) was above Naduo Cave (Table 3). For rocky desertification areas, the relatively high plant $\delta^{13}C$ is mainly because of the Gramineae plants *Imperata cylindrica*, *Capillipedium assimile*, *Arthraxon hispidus* and *Arthraxon hispidus* (Supplementary Tables 2, 3 and 4), which had $\delta^{13}C$ values as high as −11 ‰ to −13 ‰. Excepting these Gramineae plants, the average plant $\delta^{13}C$ values for the rocky desertification areas were −26.3 ‰, −29.4 ‰, and −27.7 ‰ for Guanling County, Liuzhi Special District and Panxian County, respectively. Considering the relatively small proportion (< 3 %) of biomass formed by the Gramineae plants, their contribution to the average $\delta^{13}C$ of local plants will be negligible.

In summary, based on the findings of this study, at present the dominant plants in the karst regions of Southwest China belong to C3 vegetation, characterized by negative plant $\delta^{13}C$ values of below −26 ‰ (Table 3). The regional deviation of plant $\delta^{13}C$ values was attributed to the variation of species and local environment (O'Leary, 1988).

For these five karst regions (Fig. 1), the average $\delta^{13}C_{SOM}$ value was around −19.9 ‰ to −21.5 ‰, except for above Yangkou Cave, where the average $\delta^{13}C_{SOM}$ value was −24.6 ‰ (Table 3). This relatively lower $\delta^{13}C_{SOM}$ value was attributed to the higher altitude and lower temperature, which can depress the decomposition of organic matter. It is significant that, in spite of the $\delta^{13}C$ differences of local plants, or the situation of RDD, the $\delta^{13}C_{SOM}$ values were consistent across the four regions.

The most significant changes were in the DIC-$\delta^{13}C$ of drip waters and the $\delta^{13}C$ of modern deposits in caves (Table 3). The DIC-$\delta^{13}C$ of drip waters is influenced by multiple factors, including the type of local vegetation (C3 or C4) (Cerling, 1984; McDermott, 2004), biomass, root respiration and microbial activity (Luo et al., 2007), local precipitation and humidity, residence time of soil water and its influence on dissolution of soil CO_2 (Baker et al., 1997), prior calcite precipitation (PCP) in the epikarst zone (Fairchild et al., 2006), dissolution of bedrock (Genty et al., 2001; Fairchild et al., 2006), and the openness of the karst system (Hendy, 1971; Salomons and Mook, 1986, p. 241–269). For all the sites mentioned in this study, the average $\delta^{13}C$ of bedrock ranged from −1.1 ‰ to 3.9 ‰ (Table 3). The average DIC-$\delta^{13}C$ of drip waters ranged from −11.1 ‰ to −3.0 ‰ and the average $\delta^{13}C$ of cave "modern deposits" ranged from −10.5 ‰ to −6.5 ‰ (Table 3).

There appeared to be a positive correlation between the $\delta^{13}C$ of DIC "modern deposits" and the $\delta^{13}C$ of bedrock. The DIC-$\delta^{13}C$ of drip water and the $\delta^{13}C$ of "modern deposits" changed with amplitudes of 11 ‰ and 3 ‰, respectively, in Yangkou Cave, and 11 ‰ and 4 ‰, respectively, in Naduo Cave (Fig. 9; Table 2; and Shen et al., 2016). Dissolution of bedrock is a minor contributor to the relatively small proportion of carbon in DIC (Genty, et al., 2001), and most of the carbon originates from organic sources. Furthermore, the dissolution of bedrock is also partly affected by the degree of exposure of the karst system (Hendy, 1971; Salomons and Mook, 1986, p. 241–269; Fairchild et al., 2006). For Furong, Yangkou and Naduo Caves, the different $\delta^{13}C$ values of DIC and "modern deposits" were attributed to the different RDD of these sites (Table 1), but not because of the differences in species of local plants, nor the $\delta^{13}C$ of local plants and SOM (Table 3). The RDD above Yangkou Cave and Naduo Cave are classified as No Rocky Desertification and Light Rocky Desertification, respectively (Table 1) (Xiong et al., 2002, Jiang et al., 2014). In general, the higher RDD means more rock exposure, and less soil thickness and vegetation coverage (Xiong et al., 2002, Jiang et al., 2014), resulting in less organic matter (with negative $\delta^{13}C$ values of C3 vegetation) supplied to soils. More importantly, higher RDD can lead to less bioactivity in soils, more soil erosion, and rapid infiltration of precipitation, so that an equilibrium between soil water and soil CO_2 cannot be reached (Baker et al., 1997). The above-mentioned processes lead to the relatively high $\delta^{13}C$ of drip water DIC and corresponding speleothems.

Implications for Paleoenvironment Reconstruction

Based on Cerling's (1984) findings, speleothem $\delta^{13}C$ is also interpreted to reflect the evolution of local vegetation (Coplen et al., 1994; Bar-Matthews et al., 1997; Dorale et al., 1998; Lee-Thorp et al., 2001; Genty et al., 2003; Holmgren et al., 2003; Cosford et al., 2009; Zhao et al., 2016). Undoubtedly, evolution of vegetation (C3 and C4 or the proportion of C3/C4) will change the biomass and the $\delta^{13}C$ of SOM and soil CO_2. Evolution of local vegetation is dominated by changes in temperature and precipitation (or humidity), which can directly connect the $\delta^{13}C$ of SOM and soil CO_2 with climate change. Meanwhile, there are complex processes linking soil CO_2 to speleothems, including the dissolution of soil CO_2 in vadose water (Baker et al., 1997; Bar-Matthews et al., 2000), dissolution of bedrock (Genty et al., 2001), migration of water in the vadose zone (Dreybrodt and Schloz, 2011), prior calcite precipitation (PCP) (Fairchild et al., 2006), ventilation in caves and degassing of CO_2 from drip water in relation to the CO_2 concentration of the cave atmosphere (Spötl, et al., 2005; Li et al., 2012). These processes may change the $\delta^{13}C$ values significantly and even mask the signals of local vegetation and climate. Despite this, some processes are essentially influenced by climate change. For example, higher temperatures and/or decreased precipitation, resulting from climate change, will strengthen evaporation in fractures, bringing about PCP and ultimately increased $\delta^{13}C$ in drip water and corresponding speleothems. In this situation, the $\delta^{13}C$ of speleothems can display a positive correlation with local temperature (Martin-Chivelet et al., 2011).

Variations in stalagmite $\delta^{13}C$ have been used to reconstruct the evolution of local vegetation and to assess the history of rocky desertification in the karst regions of Southwest and Central China. Lower $\delta^{13}C$ values have been interpreted to mean more extensive vegetation under wetter climate, and higher $\delta^{13}C$ values to indicate dry climate or the strengthening of rocky desertification (Cosford et al., 2009; Kuo et al., 2011). Mass works have demonstrated that the change in stalagmite $\delta^{13}C$ should not be explained simply by changes in vegetation because multiple factors can influence the change of stalagmite $\delta^{13}C$ (McDermott, 2004; Fairchild et al., 2006; Huang et al., 2016).

This investigation showed that for modern conditions, rocky desertification does not change the predominance of C3 vegetation, and there is no significant correlation between the $\delta^{13}C_{SOM}$ and RDD (Table 7). Consider that the annual temperature decreased by ~3 °C in Central China during the Oldest and Younger Dryas and Last Glacial period (Zhu et al., 2008; Caley et al., 2014), and the $\delta^{13}C$ of organic matter and pollen in peat from Southern China showed the dominance of C3 vegetation, even during cold epochs such as the Younger Dryas and Heinrich event 1 (Zhou et al., 2004; Zhong et al., 2010), the prominent enrichment trend of stalagmite $\delta^{13}C$ since the Last Glacial period in Central and Southern China, cannot be attributed to the transition of vegetation types from C3 to C4. Rocky desertification cannot necessarily change the dominance of C3 vegetation in Southern/Southwestern China, but it can change the biomass and microbial processes in soils, which then influence the $\delta^{13}C$ of speleothems (Luo et al., 2007).

Essentially, higher RDD may lead to more exposure of rock (Xiong et al., 2002; Jiang et al., 2014), less vegetation density and biomass, decreased soil thickness (Fig. 1), faster water infiltration and more soil erosion (Jiang et al., 2014). These processes reduce isotopic equilibrium between soil CO_2 and water (Baker et al., 1997; Bar-Matthews et al., 2000), increase the relative proportion of atmospheric CO_2 in soils (Genty et al., 2001), strengthen PCP in fractures (Fairchild et al., 2006), and finally result in isotopically higher $\delta^{13}C$ in DIC and speleothems. So, it is plausible that variations of stalagmite $\delta^{13}C$ in the subtropical karst regions of China reflect the soil humidity balance associated with regional hydrological circulation (Li, 2007; Liu et al., 2016), which may originate from climate change or the evolution of rocky desertification.

It is difficult to distinguish between the contribution of human activities and natural processes to rocky desertification, especially in the past 2000 years with mixed effects of population growth, irrigation, the development of farming and industrialization, and climate changes on decadal-centennial timescales (Jiang et al., 2014). For the period before the 2 ka BP, when populations were small, the change in rocky desertification and the change of speleothem $\delta^{13}C$ should mainly be attributed to natural processes, such as the change of local hydrological circulation, caused by climate changes. Based on this assumption, see the case study below.

Speleothem $\delta^{13}C$ and $\delta^{18}O$ records from Asian monsoon regions present similar patterns on orbital timescales (Jo et al., 2014), and the strong co-variation of $\delta^{13}C$ and $\delta^{18}O$ records on centennial timescales have been attributed to the soil humidity balance (Liu et al., 2016). This indicates a correlation between local vegetation, soil CO_2 and monsoon circulation (Huang et al., 2016). Strong Asian summer monsoon (ASM) is associated with higher temperature in the northern hemisphere (Cheng et al., 2016); the increased precipitation and higher temperatures in monsoon regimes benefits the prevailing of C3 vegetation. This mechanism is a logical interpretation for the similar changes of speleothem $\delta^{13}C$ and $\delta^{18}O$ records. Southwestern China is located on the main moisture transportation pathway and is mainly influenced by the relatively simple Indian summer monsoon (ISM) (Ding and Sun, 2002; Ding and Chan, 2005). The lower speleothem $\delta^{18}O$ in Southwestern China mainly indicates strengthened summer monsoon and more local precipitation (Li et al., 2007).

Based on the climate background mentioned above, a simplified concept model to assess the relationship between speleothem $\delta^{18}O$, $\delta^{13}C$, local vegetation, and precipitation for Southwest China is proposed (Fig. 10). In this model, scenario I, strong summer monsoon generates high precipitation and, combined with warmer temperatures, is conducive to the prevalence of C3 vegetation, higher vegetation density and higher soil CO_2 concentration. Increased precipitation raises the soil humidity, provides conditions for isotopic equilibrium of carbon between soil CO_2 and water, and, finally, results in lower speleothem $\delta^{18}O$ and $\delta^{13}C$ values. In scenario II, strong summer monsoon leads to heavy precipitation, rapid infiltration of soil water and non-isotopic-equilibrium between soil CO_2 and water (Baker et al., 1997; McDermott, 2004), or enhanced weathering of host rock because of the large water flux, and, finally, results in higher speleothem $\delta^{13}C$ and lower $\delta^{18}O$ values (Bar-Matthews et al., 2000). In scenario III, relatively weak summer monsoon generates lower precipitation, resulting in lower humidity, less vegetation density (still dominated by C3 plants in Southwest China), lower soil CO_2 concentration and longer residence of water in soil and fractures. In addition, because of the decline of surface water supply, it is possible that the fractures and cracks in the epikarst zone contain less water or are even empty, leading to degassing of CO_2 and PCP, which results in higher speleothem $\delta^{13}C$ values (Fairchild et al., 2006). In scenario IV, lower temperature and precipitation depresses the growth of vegetation and soil microbial activity, thereby weakening the process of pedogenesis. The main topography in Southwest China is mountainous terrain, with limited or, even, no C-horizon (weathering crust) in karst soil profiles (Jiang et al., 2014). This ultimately leads to the reduction of adhesion and affinity between the soil and bedrock. Consequently, the soil is easily eroded by heavy rainstorms and

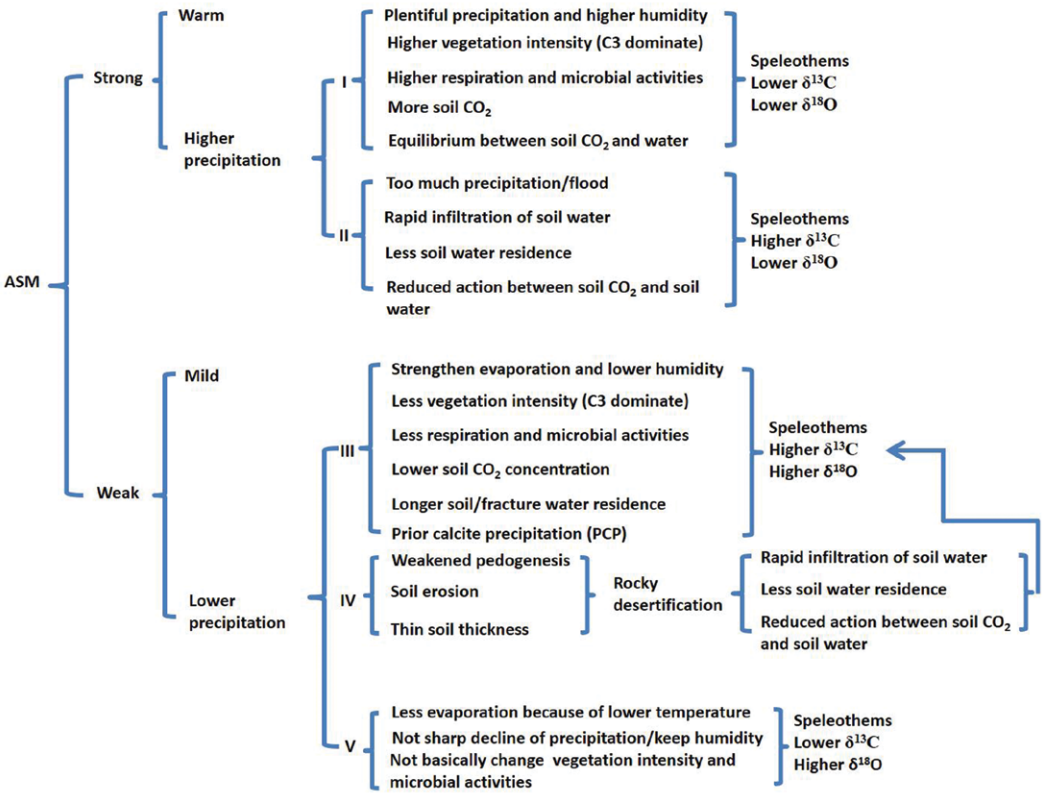

Figure 10. Concept model relating to the evolution of ASM and regional vegetation, hydrological conditions and the possible combinations of speleothem $\delta^{13}C$ and $\delta^{18}O$ in subtropical Southern and Central China.

overland flows, exposing the bedrock to rocky desertification (Yuan, 1993; Zhang et al., 2006; Jiang et al., 2014). Rocky desertification results in decreased soil thickness, rapid infiltration of surface and soil water, and non-isotopic-equilibrium between soil CO_2 and water (Baker et al., 1997; McDermott, 2004), and eventually leads to higher speleothem $\delta^{13}C$ (Fig. 10). Scenario V is also a possibility, with weak summer monsoon accompanied by mild temperatures and low precipitation (Zhu et al., 2008; Caley et al., 2014), but without reaching the threshold to trigger the transition from C3 to C4 vegetation, even over a period of decades to centuries (Zhu et al., 2008; Caley et al., 2014). Lower temperatures reduce evaporation, promote the

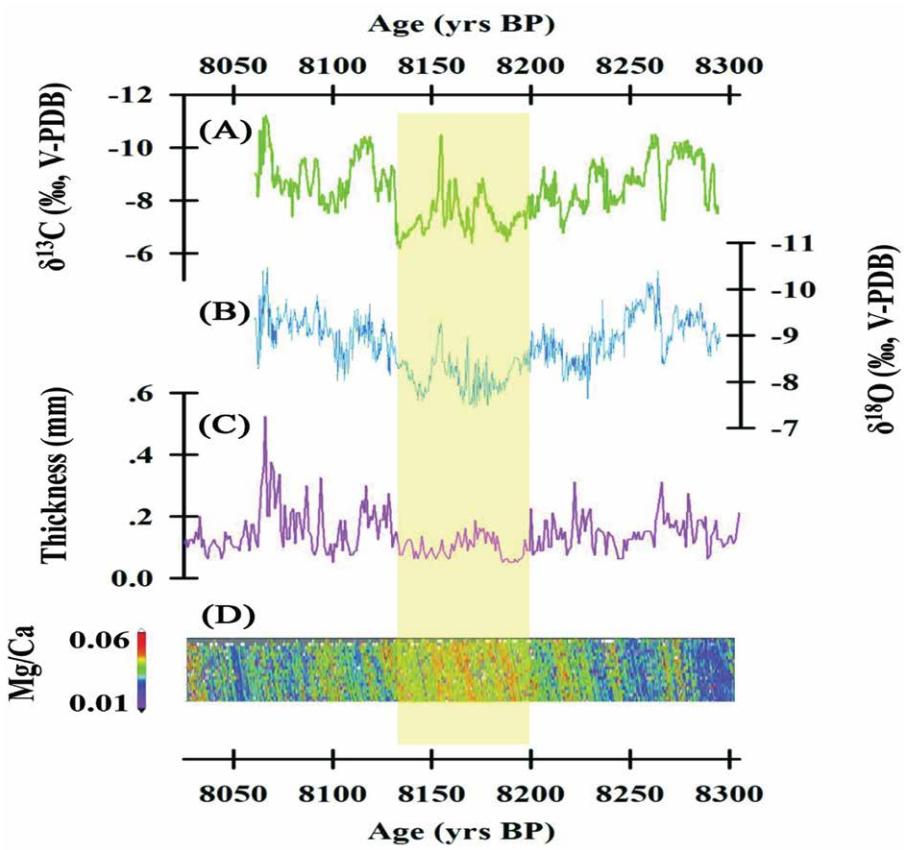

Figure 11. Comparison of multi-proxy records of stalagmite HS-4 from Heshang Cave (redrawn from Liu et al., 2013). (**A**) $\delta^{13}C$, (**B**) $\delta^{18}O$, (**C**) thickness of annual lamina, (**D**) Mg/Ca. The enriched $\delta^{13}C$ and $\delta^{18}O$ values, decreased thickness and increased Mg/Ca during the 8.2 ka event (the light-yellow bar) denoted the weakening of ASM and the possibility of PCP in the epikarst zone.

condensation of water vapor and precipitation, especially in mountainous Southwest China (Jiang et al., 2014). With this temperature and hydrology combination, Southwest China would still maintain the characteristics of a subtropical, humid monsoon climate, higher speleothem $\delta^{18}O$ and lower $\delta^{13}C$ values (Fig. 10).

It is worth pointing out that the simplified concept model comprises the abovementioned five scenarios and does not involve the complex cave factors that can cause isotopic fractionation of carbon, such as drip rate (Hansen et al., 2013), cave ventilation (Spötl et al., 2005) and degassing of CO_2 (Fairchild et al., 2006; Mickler et al., 2006; Scholz et al., 2009; Huang et al., 2016). So, speleothems from a cave with stable temperature, high humidity, poor ventilation, and that are deposited at isotopic equilibrium fractionation (Hendy, 1971), are preferential for the reconstruction of paleoclimate and paleoenvironment. In addition, the replication of speleothem records from a cave is commendatory for judging the paleoclimatic suitability of speleothems (Dorale and Liu, 2009).

Case Study for Stalagmite $\delta^{13}C$, $\delta^{18}O$, Mg/Ca and Paleoclimate

The climate- and environment-dominated organic signals carried by DIC-$\delta^{13}C$ may be masked by some inorganic and physical factors mentioned above. In such cases, the analysis of multi-proxies is recommended to assess the influences of these factors; e.g., higher Mg/Ca ratio and lower Ca^{2+} concentration in drip water have been used to reflect the PCP effect (Fairchild et al., 2006; Luo et al., 2013), and $^{87}Sr/^{86}Sr$ has been used to reflect the dissolution of host rock (Oster et al., 2010). Multi-proxy records from the same cave will undoubtedly raise the reliability of paleoclimate and paleoenvironment reconstruction. Here, a case study to demonstrate this argument is presented.

Heshang Cave is in central China (30°27' N, 110°25' E, 294 m a.s.l, ~290 km northeast of Furong Cave) (Fig. 1B), and has been monitored for more than 10 years (Hu et al., 2008a; Henderson et al., 2008). The $\delta^{18}O$ of rainwater above Heshang Cave is not altered by evaporation when it filters into the cave and stalagmite $\delta^{18}O$ has been used as the indicator for changes in rainfall (Hu et al., 2008b). As shown in Figure 11, both the sub-annually resolved $\delta^{18}O$, $\delta^{13}C$ and Mg/Ca values of stalagmite HS-4 from Heshang Cave increased significantly during the 8.2 ka event, a global cold-climatic event, which occurred at ~8.2 ka BP (Liu et al., 2013). In other words, the decrease in rainfall indicated by the increased $\delta^{18}O$ of stalagmite HS-4 was strongly supported by higher $\delta^{13}C$ and high ratios of Mg/Ca (Liu et al., 2013). This is because in Heshang Cave, lower rainfall means lower karst flow rates and more opportunity for PCP, which leads to higher stalagmite $\delta^{13}C$ and Mg/Ca (Johnson et al., 2006; Hu et al., 2008a; Henderson et al., 2008; Liu et al., 2013), as described in scenario III (Fig. 10). In contrast, lower stalagmite $\delta^{18}O$ means more rainfall, faster karst flow rates and no/less PCP, which can result in lower $\delta^{13}C$ and Mg/Ca ratio, as described in scenario I (Fig. 10).

It is known that stalagmite $\delta^{13}C$ shows significant variability and uncertainty, even in stalagmites from the same cave. There are different correlations between the $\delta^{13}C$ and $\delta^{18}O$ values for a given stalagmite on different time scales, e.g., orbital-, millennial- and centennial-scale (Liu et al., 2016). Complex factors may influence stalagmite $\delta^{13}C$, such as vegetation types and density, biomass, soil pCO_2, and karst flow rate, which are all closely associated with climate change-dominated temperature and precipitation (McDermott, 2004). Cave monitoring and multi-proxy analysis for stalagmites, including $\delta^{13}C$, $\delta^{18}O$, Mg/Ca, $^{87}Sr/^{86}Sr$, is particularly important for the reliable interpretation of $\delta^{13}C$ (Li et al., 2014b). In addition, lacustrine and peat records are a valuable source of information for subtropical Central and Southern China, because pollen records from neighboring regions can provide direct evidence for variation in regional vegetation and climate, and may provide supporting evidence for changes in local vegetation.

Conclusions

Although speleothem $\delta^{13}C$ has been used to trace the evolution of regional vegetation and rocky desertification history, there has not been a systematic investigation on the present vegetation types and isotopic composition of plants in Southern and Central China areas with humid subtropical monsoon climate. In this study, 130 plant samples were collected from five sites with different RDD in Southwest China, revealing most plants to be C3 plants. There was no correlation between the $\delta^{13}C_{SOM}$ and RDD; in contrast, the DIC-$\delta^{13}C$ of drip water and $\delta^{13}C$ of "modern deposits" in caves changed with large amplitude due to hydrological conditions in the epikarst zone and geological and physical characteristics of individual caves/drip sites. This study revealed that, at present, rocky desertification in Southwest China does not cause the transition of C3 to C4 vegetation. Additionally, based on pollen records in Southern and Central China, it was inferred that this transition did not occur during the Last Glacial period.

A concept model comprising five scenarios was proposed, indicating that the evolution of ASM and rocky desertification can be recorded in speleothem $\delta^{13}C$, mainly by the change of epikarst hydrological conditions rather than the change of vegetation types. Cave monitoring and multi-proxy analysis are recommended to identify the influence of non-climatic factors, which are believed to be instrumental in providing a reliable explanation of speleothem $\delta^{13}C$ and reconstruction of paleoenvironment.

Acknowledgements

Thank you to Mr. Huang Chuliang for his great assistance with field work in Guizhou Province. Dr. Liu Jinchun, School of Life Sciences, Southwest University, China, is greatly appreciated for identification of all plants. A profession-

al English translator, Dr. Xiang Xinyi, Southwest University, China, is also greatly appreciated for her effort in polishing the manuscript. This research was supported by NSFC (Nos. 41172165, 41440020), the Fundamental Research Funds for the Central Universities (Nos. XDJK2017A010, XDJK2013A012) to Ting -Yong Li.

References

Baker, A., Ito, E., Smart, P.L., Mcewan, R.F., 1997, Elevated and variable values of 13C in speleothems in a British cave system, Chemical Geology, v. 136, s3-4, p. 263–270.

Bar-Matthews, M., Matthews A., Sass E., Halicz L., Ayalon A., 1996, Carbon and oxygen isotope study of the active water-carbonate system in a karstic Mediterranean cave: Implications for paleoclimate research in semiarid regions, Geochimica et Cosmochimica Acta, v. 60, n. 2, p. 337–347. https://doi.org/10.1016/0016-7037(95)00395-9.

Bar-Matthews, M., Ayalon, A., Kaufman, A., 1997, Late Quaternary paleoclimate in the eastern Mediterranean region from stable isotope analysis of speleothems at Soreq Cave, Israel, Quaternary Research, v. 47, n. 2, p. 155–168. https://doi.org/10.1006/qres.1997.1883.

Bar-Matthews, M., Ayalon, A., Kaufman, A., 2000, Timing and hydrological conditions of Sapropel events in the Eastern Mediterranean, as evident from speleothem, Soreq Cave, Israel, Chemical Geology, v. 169, n. 1, p. 145–156. https://doi.org/10.1016/S0009-2541(99)00232-6.

Zhu Cheng, Xing Chen, Zhang GuangSheng, Ma ChunMei, Zhu Qing, Li ZhongXuan, Xu WeiFeng, 2008, Spore-pollen-climate factor transfer function and paleoenvironment reconstruction in Dajiuhu, Shennongjia, Central China, Chinese Science Bulletin, v. 53, p. 42–49.

Caley, T., Roche, D.M., Renssen, H., 2014, Orbital Asian summer monsoon dynamics revealed using an isotope-enabled global climate model, Nature Communications, v. 5, p. 5371. https://doi:10.1038/ncomms6371.

Cerling, T.E., 1984, The stable isotopic composition of modern soil carbonate and its relationship to climate, Earth and Planetary Science Letters, v. 71, p. 229–240. https://doi.org/10.1016/0012-821X(84)90089-X.

Hu Chaoyong, Henderson, G.M., Huang Junhua, Chen Zhenghong, Johnson, K.R., 2008a, Report of a three-year monitoring programme at Heshang Cave, Central China, International Journal of Speleology, v. 37, n. 3, p. 143–151. https://doi.org/10.5038/1827-806X.37.3.1.

Hu Chaoyong, Henderson, G.M., Huang Junhua, Xie S.C., Sun Y., Johnson, K.R., 2008b, Quantification of Holocene Asian monsoon rainfall from spatially separated cave records, Earth and Planetary Science Letters, v. 266, n. 3-4, p. 221–232.

Coplen, T.B., Winograd, I.J., Landwehr, J.M., Riggs, A.C., 1994, 500,000-year stable carbon isotopic record from Devil's Hole, Nevada, Science, v. 263, n. 5145, p. 361–365. https://doi.org/10.1126/science.263.5145.361.

Cosford, J., Hairou Qing, Mattey, D., Eglington, B., Meilang Zhang, 2009, Climatic and local effects on stalagmite $\delta^{13}C$ values at Lianhua Cave, China, Palaeogeography, Palaeoclimatology, Palaeoecology, v. 280, n. 1, p. 235–244. https://doi.org/10.1016/j.palaeo.2009.05.020.

Yuan Daoxian, 1993, Environmental change and human impact on karst in south China, *in* Williams, P., ed., Karst terrains: environmental change and human impact, Catena Supplement, v. 25, p. 104.

Yuan Daoxian, 1997, Rock desertification in the subtropical karst of south China, Zeitschrift fur Geomorphologie, n. 108, p. 81–90.

Liu Dianbing, Wang Yongjin, Cheng Hai, Edwards R.L., Kong Xinggong, Li Ting-Yong, 2016, Strong coupling of centennial-scale changes of Asian monsoon and soil processes derived from stalagmite $\delta^{18}O$ and $\delta^{13}C$ records, southern China, Quaternary Research, v. 85, n. 3, p. 333–346.

Dienes, P., 1980, The isotopic composition of reduced organic carbon, *in* Fritz, P., Fontes, J. C., eds., Handbook of Environmental Isotope Geochemistry I: The Terrestrial Environment, Amsterdam: Elsevier.

Dorale, J.A., González, L.A., Reagan, M.K., Pickett, D.A., Murrell, M.T., Baker, R.G., 1992, A high-resolution record of Holocene climate change in speleothem calcite from Cold Water Cave, northeast Iowa, Science, v. 258, p. 1626–1630. https://doi.org/10.1126/science.258.5088.1626.

Dorale, J.A., Edwards, R.L., Emi, I., Gonzalez, L.A., 1998, Climate and vegetation history of the midcontinent from 75 to 25 ka: A speleothem record form Crevice Cave, Missouri, USA, Science, v. 282, p. 1871–1874. https://doi.org/10.1126/science.282.5395.1871.

Dorale J, Liu Zaihua, 2009, Limitations of Hendy Test criteria in judging the paleoclimatic suitability of speleothems and the need for replication, Journal of Cave and Karst Studies, v. 71, n. 1, p. 73–80.

Dreybrodt, W., Scholz, D., 2011, Climatic dependence of stable carbon and oxygen isotope signals recorded in speleothems: From soil water to speleothems calcite, Geochimica et. Cosmochimica Acta, v. 75, n. 3, p. 734–752. https://doi.org/10.1016/j.gca.2010.11.002.

Fairchild, I.J., Smith, C.L., Baker, A., Fuller, L., Spötl, C., Mattey, D., McDermott, F., E.I.M.F., 2006, Modification and preservation of environmental signals in speleothems, Earth Science Reviews, v. 75, p. 105–153. https://doi.org/10.1016/j.earscirev.2005.08.003.

Frisia, S., Fairchild, I.J., Fohlmeister, J., Miorandi, R., Spötl, C., Borsato, A., 2011, Carbon mass-balance modeling and carbon isotope exchange processes in dynamic caves, Geochimica et Cosmochimica Acta, v. 75, n. 2, p. 380–400. https://doi.org/10.1016/j.gca.2010.10.021.

Genty, D., Baker, A., Massault, M., Proctor, C., Gilmour, M., Pons-Branchu, E., Hamelin, B., 2001, Dead carbon in stalagmites: carbonate bedrock paleodissolution vs. ageing of soil organic matter: Implications for ^{13}C variations in speleothems, Geochimica et Cosmochimica Acta, v. 65, n.20, p. 3443–3457. https://doi.org/10.1016/S0016-7037(01)00697-4.

Genty, D., Blamart, D., Ouahdi, R., Gilmour, M., Baker, A., Jouzel J., Van-Exter, S., 2003, Precise dating of Dansgaard-Oeschger climate oscillations in western Europe from stalagmite data, Nature, v. 421, p. 833–837. https://doi.org/10.1038/nature01391.

Cheng Hai, Edwards, R. L., Sinha Ashigh, C. Spötl, Yi Liang, Chen Shitao, Kelly, M., Gayatri Kathayat, Wang Xiangfeng, Li Xianglei, Kong Xinggong, Wang Yongjin, Ning Youfeng, Zhang Haiwei, 2016, The Asian monsoon over the past 640,000 years and ice age terminations, Nature, v. 534, p. 640–646. https://doi.org/10.1038/nature18591.

Hansen, M., Dreybrodt, W., Scholz, D., 2013, Chemical evolution of dissolved inorganic carbon species flowing in thin water films and its implications for (rapid) degassing of CO_2 during speleothem growth, Geochimica et Cosmochimica Acta, v 107, p. 242–251. https://doi.org/10.1016/j.gca.2013.01.006.

Wang H.-B, Li Ting-Yong, Yuan N., Li J.-Y., 2014, Environmental signification and characteristics of δD and δ18O variation in drip water in Yangkou Cave, Chongqing, Carsologica Sinica, v. 33, n. 2, p. 146–155. (In Chinese with English abstract and figures).

Henderson, G.M., Hu C.Y,. Johnson, K. R., 2008, Controls on trace elements in stalagmites derived from *in situ* growth in a Chinese cave, 18th Annual V M Goldschmidt Conference A 366.

Hendy, C.H., 1971, The isotopic geochemistry of speleothems: The calculation of the effects of different modes of formation on the isotopic composition of speleothems and their applicability as palaeoclimatic indicators, Geochimica et Cosmochimica Acta, v. 35, n. 8, p. 801–824. https://doi.org/10.1016/0016-7037(71)90127-X.

Holmgren, K., Lee-Thorp, J.A., Cooper, G.R.J., Lundblad, K., Partridge, T.C., Scott, L., Sithaldeen, R., Talma, A.S., Tyson, P.D., 2003, Persistent millennial-scale climatic variability over the past 25,000 years in southern Africa, Quaternary Science Review, v. 22, n. 21-22, p. 2311–2326. https://doi.org/10.1016/S0277-3791(03)00204-X.

Li Hong Chun, Gu D.L., Chen W.J., Yuan Daoxian, Li Ting-Yong, 1998, Application of high-resolution carbon isotope record of a stalagmite from the Shihua Cave, Beijing— $\delta^{13}C$ record of deforestation after the establishment of the Grand Capital (Yuan Dadu) in 1272 A. D., Geological Review, v. 44, n. 5, p. 456–463 (In Chinese with English abstract). http://baike.baidu.com/l/R39lSAyx?bk_share=copy.
https://baike.baidu.com/item/%E5%A4%A7%E7%94%A8%E9%95%87/32613.

Xiong K.N., Li P., Zhou Z.F., An Y.L., Lv T., Lan A.J., 2002, Remote sensing of rocky desertification in karst: a case study of Guizhou Province: Geological Publishing House, v. 23.

Jo Kyoung-ham, Woo Kyung Sik, Sangheon Yi, Yang Dong-Yoon, Lim Hyoun Soo, Wang Yongjin, Cheng Hai, Edwards, R.L., 2014, Mid-latitude interhemispheric hydrologic seesaw over the past 550,000 years, Nature, v. 508, p. 378–382. https://doi.org/10.1038/nature13076.

Johnson, K. R., Hu Chaoyong, Belshaw, N.S., Henderson, G.M., 2006, Seasonal trace-element and stable-isotope variations in a Chinese speleothem: The potential for high-resolution paleomonsoon reconstruction, Earth and Planetary Science Letters, v. 244, n. 1-2, p. 394–407. https://doi.org/10.1016/j.epsl.2006.01.064.

Lee-Thorp, J.A., Holmgren, K., Lauritzen, S.-E., Linge, H., Moberg, A., Partridge, T.C., Stevenson, C., Tyson, P.D., 2001, Rapid climate shifts in the southern African interior throughout the mid to late Holocene, Geophysical Research Letters, v. 28, p. 4507–4510. https://doi.org/10.1029/2000GL012728.

Martín-Chivelet, J., Muñoz-García, M.B., Edwards, R.L., Turrero, M.J., Ortega, A.I., 2011, Land surface temperature changes in Northern Iberia since 4000 yr BP, based on $\delta^{13}C$ of speleothems, Global Planetary Change, v. 77, n. 1-2, p. 1–12. https://doi.org/10.1016/j.gloplacha.2011.02.002.

Mattey, D.P., Atkinson, T.C., Barker, J.A., Fisher, R., Latin, J.P., Durrell, R., Ainsworth M., 2016, Carbon dioxide, ground air and carbon cycling in Gibraltar karst, Geochimica et Cosmochimica Acta, v. 184, p. 88–113. https://doi.org/10.1016/j.gca.2016.01.041.

McDermott, F., 2004, Palaeo-climate reconstruction from stable isotope variations in speleothems: a review, Quaternary Science Review, v. 23, n. 7, p. 901–918. https://doi.org/10.1016/j.quascirev.2003.06.021

Zhang Meilang, Zhu X.Y., Lin Y.S., Qin J.M., Zhang C., Luo R.G., Yang Y., 2006, Study on$\delta^{13}C$ isotope records from stalagmites, Guangxi Sciences. https://doi.org/10.3969/j.issn.1005-9164.2006.01.016.

Mickler, P.J., Stern, L.A., Banner, J.L., 2006, Large kinetic isotope effects in modern speleothems, Geological Society of America Bulletin, v. 118, n. 1/2, p. 65–81. https://doi.org/10.1130/B25698.1.

Zhao Min, Li Hong-Chun, Shen Chuan-Chou, Kang Su-Chen, Chou Chun-Yen, 2016, $\delta^{18}O$, $\delta^{13}C$, elemental content and depositional features of a stalagmite from Yelang Cave reflecting climate and vegetation changes since late Pleistocene in central Guizhou, China, Quaternary International. https://doi.org/10.1016/j.quaint.2016.07.022.

O´Leary, M.H., 1988, Carbon isotope in photosynthesis, Bioscience, v. 38, n. 5, p. 328–336.

Oster, J.L., Montañez, I.P., Guilderson, T.P., Sharp, W.D., Banner, J.L., 2010, Modeling speleothem $\delta^{13}C$ variability in a central Sierra Nevada cave using ^{14}C and $^{87}Sr/^{86}Sr$, Geochimica et Cosmochimica Acta, v. 74, n. 18, p.5228–5242.

Salomons, W., and Mook, W.G., 1986, Isotope geochemistry of carbonates in the weathering zone: The Terrestrial Environment B. Elsevier B.V.

Scholz, D., Mühlinghaus, C., Mangini, A., 2009, Modelling $\delta^{13}C$ and $\delta^{18}O$ in the solution layer on stalagmite surfaces, Geochimica et Cosmochimica Acta, p. 73, n. 9, p. 2592–2602.

Spötl, C., Fairchild, I.J., Tooth, A.F., 2005, Cave air control on drip water geochemistry, Obir Caves (Austria, p. implications for speleothem deposition in dynamically ventilated caves, Geochimica et Cosmochimica Acta, v. 69, p. 2451–2468.

Li Ting-Yong, 2007, The controlling factors research on the paleoenvironmental informations in stalagmite and the paleoclimate reconstruction since the last glacial period in Chongqing area, [Ph.D. dissertation]: Chongqing, China, Southwest University.

Li Ting-Yong, Daoxian Yuan, Li Hong Chun, Yangyan, Wang Jianli, Wang, Xinya, Li, Jun-Yun, Qin, Jiaming, Zhang, M Meilang, Lin, Yushi, 2007, High-resolution climate variability of southwest China during 57-70 ka reflected in a stalagmite $\delta^{18}O$ record from Xinya Cave, Science China Earth Sciences, v. 50, n. 8, p. 1202–1208. https://doi.org/10.1007/s11430-007-0059-z.

Li Ting-Yong, Shen Chuan-Chou, Li Hong Chun, Li Jun-Yun, Chiang Hong-Wei, Song Sheng-Rong, Yuan Daoxian, Chris D.-J., Gao LinPan, Zhou Liping, Wang Jian Li, Yang Ye Ming, Tang Liang-Liang, Xie Shi-You, 2011, Oxygen and carbon isotopic systematics of aragonite speleothems and water in Furong Cave, Chongqing, China, Geochimica et Cosmochimica Acta, v. 75, p. 4140–4156. https://doi.org/10.1016/j.gca.2011.04.003.

Li Ting-Yong, Li Hong Chun, Xiang Xiao, Kuo TzShing, Li Jun Yan, Zhou Fu Li, Chen Hong Li, Peng Ling Li, 2012, Transportation characteristics of $\delta^{13}C$ in the plants-soil-bedrock-cave system in Chongqing karst area, Science China Earth Sciences, v. 55, n. 4, p. 685–694. https://doi.org/10.1007/s11430-011-4294-y.

Li Ting-Yong, Shen Chuan-Chou, Huang L.-J., Jiang X.-Y., Yang X.-L., Mii H.-S., Lee S.-Y., and Lo L., 2014a, Stalagmite-inferred variability of the Asian summer monsoon during the penultimate glacial–interglacial period, Climate of the Past, v. 10, p. 1211–1219. https://doi.org/10.5194/cp-10-1211-2014.

Kuo Tz-Shing, Liu Zi-Qi, Li Hong-Chun, Wan Nai-Jung, Shen Chuan-Chou, Ku The-Lung, 2011, Climate and environmental changes during the past millennium in central western Guizhou, China as recorded by Stalagmite ZJD-21, Journal of Asian Earth Sciences, v. 40, n. 6, p. 1111–1120. https://doi.org/10.1016/j.jseaes.2011.01.001.

Trumbow, S., 2000, Age of soil organic matter and soil respiration: radiocarbon constraints on below-ground c dynamics, Ecological Applications, v. 10, n. 2, p. 399–411. https://doi.org.10.1890/1051-0761.

Liu Y. H., Henderson, G.M., Hu ChaoYong, Mason, A.J., Charnley, N., Johnson, K. R., Xie S.–C., 2013, Links between the East Asian monsoon and North Atlantic climate during the 8,200-year event, Nature Geoscience, v. 6, p. 117–120. https://doi.org/10.1016/j.yqres.2016.02.008.

Huang W., Dianbing Liu, Wang Yongjin, Zhang Z.Q., 2016, Research status and advance in carbon isotope ($\delta^{13}C$) variation from stalagmite, Advances in Earth Science, v. 31, n. 9, p. 968–983. (In Chinese with English Abstract)

Zhou Weijan, Yu Xuefeng, Jull, A.J.T., Burr, G., Xiao J.Y., Lu Xuefeng, Xian Feng, 2004, High-resolution evidence from Southern China of an early Holocene optimum and a mid-Holocene dry event during the past 18,000 years, Quaternary Research, v. 62, p. 39−48.

Luo Weijun, Wang S.J., Liu X.M., 2007, Biomass effect on carbon isotope ratios of modern calcite deposition and its mechanism: A case study of four caves in Guizhou Province, China, Geochimica, v. 36, n. 4, p. 344–350. (In Chinese with English Abstract)

Luo Weijun, Wang S.J., 2009, Transmission of $\delta^{13}C$ signals and its paleoclimatic implications in Liangfeng Cave system of Guizhou Province, SW China, Environmental Earth Science, v. 59, p. 655–661. https://doi.org/10.1007/s12665-009-0062-0.

Luo Weijun, Wang S., Xie X., Zhou Y., Li Ting-Yong, 2013, Temporal and spatial variations in hydrogeochemistry of cave percolation water and their implications for four caves in Guizhou, China, China Journal of Geochemistry, v. 32, n. 2, p. 119–129. https://doi.org/10.1007/s12665-009-0062-0.

Shen W., Wang J.L., Jiang X.S., Mao Q.Y., 2016, Hydrochemistry and $\delta^{13}C_{DIC}$ features of cave water in Naduo Cave, Guizhou and their influencing factors, Carsologica Sinica, v. 35, n. 1, p. 98–105. (In Chinese with English abstract)

Zhong Wei, Xue Jibin, Zheng Yonming, Ma Qiaohong, Cai Ying, Ouyang Jun, Xu Liubin, Zhou Shangzhe, Yu Xuefeng, 2010, Variations of monsoonal precipitation over the last 16,000 years in the eastern Nanling Mountains, South China, Journal of Paleolimnology, v. 44, p. 177–188.

Ding Yihui, Sun Y., 2002, Seasonal march of the East Asian summer monsoon and related moisture transport, Weather and Climate, v. 1, p. 18–23. (In Chinese with English Abstract)

Ding Yihui, Chan Johnny C.L., 2005, The East Asian summer monsoon: an overview, Meteorology and Atmospheric Physics, v. 89, p. 117–142. https://doi.org/10.1007/s00703-005-0125-z.

Li Z.H., Driese, S.G., Cheng Hai, 2014b, A multiple cave deposit assessment of suitability of speleothem isotopes for reconstructing palaeo-vegetation and palaeo-temperature, Sedimentology, v. 61, n. 3, p. 749–766. https://doi.org/10.1111/sed.12078.

Jiang Zongcheng, Lian Yanqing, Qin Xqaoqun, 2014, Rocky desertification in southwest china: impacts, causes, and restoration, Earth Science Review, v. 132, n. 3, p. 1–12. https://doi.org/10.1016/j.earscirev.2014.01.005.